Universidade de Lisboa

FACULDADE DE CIÊNCIAS

DEPARTAMENTO DE BIOLOGIA VEGETAL

Proteomics study of the effect of heavy metals - induced stress in transgenic tobacco plants, with different expression levels of trehalose-6-phosphate synthase.

Luis Filipe Pinheiro Domingues

Master in Biologia Celular e Biotecnologia

2012

Universidade de Lisboa

FACULDADE DE CIÊNCIAS

EPARTAMENTO DE BIOLOGIA VEGETAL

Proteomics study of the effect of heavy metals - induced stress in transgenic tobacco plants, with different expression levels of trehalose-6-phosphate synthase

Luis Filipe Pinheiro Domingues

Master in Biologia Celular e Biotecnologia

Thesis oriented by Professor Jorge Silva and André Almeida PhD

2012

Do not hesitate to leap in the abyss because is only when you fall that you learn whether you can fly

Acknowledgements

First of all, I would like to thank Professor Ana Varela Coelho for giving me the opportunity to work in the Mass Spectrometry lab and in this particular subject of research. I also thank André Almeida for the support and guidance during the time I was working in this project.

To the project PTDC/AGR-AAM/102821/2008 - Plant responses to trace element toxicity: cellular mechanisms for detoxification and tolerance, in the person of Miguel Mourato and Luisa Louro, for the opportunity of participate in it.

And to the team who transformed the Tobacco plants used in this work, namely André Almeida, Susana Araujo, Dulce Santos e Pedro Fevereiro among others.

I want also to thank my parents and my brother for all the unconditional support through all my life

To Sofia Trindade who always supported me and talked my ear off anytime I needed. A sincerely thank you.

To Beta, Renata and Cat, for all the support and quick tips in the lab. Above all know that you became friends rather than co-workers.

To Rita Laires and Joana Martins, my fellow MSc student for hear my whining when the something went wrong

I dedicate this thesis to all my friends, new or old

Abstract

Presently, heavy metal contamination is an important pollution problem in world agriculture. The specific issues concerning heavy metal, in farming issues, are mainly due to their accumulation in the food chain with direct consequences to the consumer health. Cadmium (Cd), particularly, is one of the most challenging pollutants, due to its high water solubility, mobility, persistence and toxicity, even in low concentrations.

Trehalose is a sugar that acts as an osmoprotector, and has the capacity to stabilize membranes and proteins during desiccation, heat and osmotic stress. Trehalose-6-phosphate synthase, one of the enzymes of the biosynthetic pathway has been the major target for genetic engineering, as it is considered to be the decisive factor in the trehalose biosynthesis.

The aim of the present work is to study the effects of a Cd exposure of two transgenic *Nicotiana tbacum* lines (B5H and B1F), which had already shown enhanced tolerance to abiotic stress, in comparison to wild type. We used a proteomics approach, namely 2-DE-DIGE.and identification of differentially expressed proteins by mass spectrometry.

In this work we could identify fifteen different proteins, such as carbonic anhydrase, RuBisCO and phosphoglycerate kinase, with differential expression. Results demonstrate that both B1F and B5H present an enhanced tolerance to cadmium induced stress, showing signals which denote that they may not be as affected as Wt plants by the concentration of cadmium to which they were subjected. The physiological significance of the expression profiles obtained is discussed. Genetic engineering with the trehalose-6-phosphate synthase gene seems therefore to be of use in obtaining transgenic plants of commercial use for possible growth in contaminated soils or used in phytoremediation.

Keywords: *Nicotiana tbacum*; Trehalose-6-phosphate synthase; AtTPS1; 2-DE; DIGE; Mass Spectrometry; MALDI-TOF/TOF.

Resumo alargado

A contaminação dos solos por metais pesados é um importante problema ambiental. Um dos principais problemas da contaminação de solos agrícolas prende-se com a acumulação destes metais na cadeia alimentar com consequências directas, graves, na saúde do consumidor. O Cádmio (Cd), em particular, é um dos poluentes mais problemáticos, devido à sua elevada solubilidade em água, mobilidade, persistência e toxicidade, mesmo em baixas concentrações.

A trealose é um açúcar que actua como osmoprotector e tem a capacidade de estabilizar membranas e proteínas durante stresses provocados por dissecação, temperatura, e stress osmótico. A Trealose-6-fosfato-sintase, uma das enzimas da via biossintética da trehalose tem sido o alvo principal para a engenharia genética, uma vez que é considerado o factor determinante na biossíntese de trealose..

Com o presente trabalho pretende-se, utilizando uma abordagem proteómica, baseada em 2-DE-DIGE seguida de identificação de proteínas por espectrometria de massa, estudar os efeitos da uma exposição a Cd em duas linhas de *Nicotiana tbacum* (B5H e B1F), que já tinham demonstrado tolerância aumentada a stress abiótico induzido por metais pesados, em comparação com plantas Wild type.

Neste trabalho foi possível identificar 15 proteínas diferentes, tais como a anhidrase carbónica, a RuBisCO e a fosfoglicerato kinase, com expressão diferencial. Os resultados demonstram que tanto as plantas B1F como as B5H apresentam uma tolerância aumentada ao stresse induzido por cádmio., mostrando sinais que denotam que eles podem não ser tão afetado quanto plantas Wt pela concentração de cádmio a que foram submetidas. O significado fisiológico dos perfis de expressão obtidos é discutido. A engenharia genética com o gene da sintetase de trealose-6-fosfato parece, portanto, ser util na obtenção de plantas transgénicas de uso comercial para uma possível plantação em solos contaminados ou utilizados em fitorremediação.

Palavras-chave: *Nicotiana tbacum*; Trehalose-6-fosfate synthase; AtTPS1; 2-DE; DIGE; Mass Spectrometry; MALDI-TOF/TOF.

Index

Index of figures

1 Introduction

1.1 Heavy metals

1.1.1 Contamination and contamination sources

Soil heavy metal contamination has been one of the major concerns due to their toxicity, persistence and non-degradability in the environment. Presently, heavy metal contamination is a major world agricultural problem. The specific issues regarding heavy metal, in agricultural environment, are mainly due to their accumulation in the food chain with direct consequences to the consumer health[1,2]. For this reason the development of economically feasible remediation techniques represents a pressing technological and scientific issue. Several crops plant present the advantage of accumulating metals, if grown on metal polluted soil or irrigated with polluted water, being therefore a good tool for phytoremediation[3,4].

Trace elements like heavy metals are important contaminants that occur in consequence of human activities[5,6]. The contamination of fields with these elements increased radically since the Industrial Revolution. The main sources of contamination are activities like mining and smelting, municipal wastes, industry, but also agriculture due to the use of fertilizers and pesticides[6]. Despite the fact that several heavy metals like Iron, Zinc and Copper are essential for plant physiology as micronutrients and only in high levels became toxic, there are others, like Arsenic, Lead, Cadmium and Mercury, that are non essential and highly toxic even in low concentrations[7].

The presence of these contaminants can affect plant growth and development. Once heavy metal concentration increased in the plant cytosol, it becomes harmful, inhibiting transpiration and photosynthesis, disturbing carbohydrate metabolism, and driving to secondary stresses like nutrition and oxidative stresses, which collectively affect plant development and growth and consequently in agricultural crops, their yields and their safe consumption. The toxic dose depends on several factors, in particular the type and concentration of the ion, plant species, and the stage of plant growth, among others [6–8]

Cadmium (Cd), in particular, is one of the most problematic pollutants, due to its high water solubility, mobility, persistence and toxicity, even in low concentrations.

Cadmium is released into the environment in large amounts, usually through man-made factors and animals and humans are exposed to it via the ingestion of contaminated food, leading to health problems namely renal tubular dysfunction and cancer[9–11].

Albeit the high phytotoxicity, Cd is easily taken up by plant roots and transported to aerial tissues. Being highly mobile in the phloem, Cd can be accumulated in all plant parts which cause disruption of physiological processes, inhibits photosynthesis, inactivates enzymes in CO_2 fixation, induces lipid peroxidation, inhibits pollen germination and tube growth, and also disturbs the nitrogen (N) and sulfur (S) metabolism and antioxidant machinery; leading to leaf chlorosis, root necrosis and stunted growth [10–13].

Cd can be taken up by roots via Fe or Zn transporters while interfering with the uptake, transport, and use of others elements such Ca, Mg, P, and K. As soon as it is translocated to the shoots, it alters chlorophyll content, photochemical quantum yield of photosynthesis light harvesting complex I and II and other photosynthetic processes[14].

Plants respond to avoid harmful effects in a variety of different ways. This tolerance to metals is based on multiple mechanisms such as cell wall binding, compartimentation in the vacuoles by active transport of ions mediated by transporter proteins, and the chelation of ions by forming of complexes with organic acids or peptides phytochelatins. Components of this network have been identified continuously, mainly through proteomic analysis of the protein expression pattern variations[6–8,15].

1.2 Trehalose

1.3 Role in plants

Trehalose is a sugar discovered, in 1832 by Wiggers, in the sequence of the research over rye's ergot[16]. The name trehalose was introduced in 1858, because it was found in coccons of desert beatles named "trehala" by Berthelot[16,17]. Since then, its effects in organisms have been widely studied[18]. In plants, trehalose presence was discovered very recently, particularly in plants tolerant to desiccation and generally termed "resurrection plants" like the fern *Selaginella lepidophylla* [19]. Trehalose is a

disaccharide, containing two units of D-glucose, linked in a α,α-1,1 configuration, as shown in Figure 1; is a nonreducing sugar, not easily hydrolyzed by acid and resistant to cleavage by α-glucosidase[16–18,20].

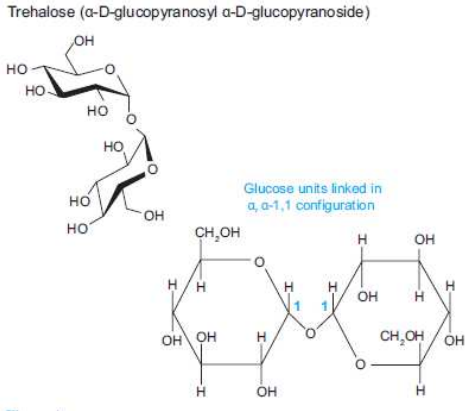

Figure 1: Trehalose molecule (adapted from Paul, et al, 2008)

The molecule occurs in a large range of organisms besides plants: fungi, bacteria, yeasts, algae, insects and other invertebrates and its role in the metabolism of these organisms can be diverse[18], but the most important known activity of trehalose is the capacity to enhance the tolerance of plants to abiotic stress, namely water deficit stress. Acting as an osmoprotector, trehalose has the capacity to stabilize membranes and proteins during desiccation, heat and osmotic stress [16,21,22]. Due to its characteristics, trehalose is a potential target for genetic engineering in plants, towards the enhancement of abiotic stress tolerance.

1.3.1 Biosynthesis pathway

There are five trehalose biosynthetic pathways known in living organisms and there are organisms with various pathways and others with just one[15], but in eukaryotic organisms only one pathway in known[23]. Such pathway consists in two steps, in the first one UDP-Glucose and Glucose-6-phosphate are linked, in a reaction catalyzed by the enzyme trehalose-6-phosphate synthase (TPS), and then in the second step, trehalose-6-phosohate phosphatase (TPP) removes the phosphate group, resulting in free trehalose. Trehalose can be cleaved by the enzyme trehalase, into two molecules of glucose (**Erro! A origem da referência não foi encontrada.**)[16,22,23]. TPS is the major target for genetic engineering, because it is considered to be the critical factor in the trehalose biosynthesis, since TPP can be replaced by endogenous phosphatases[22].

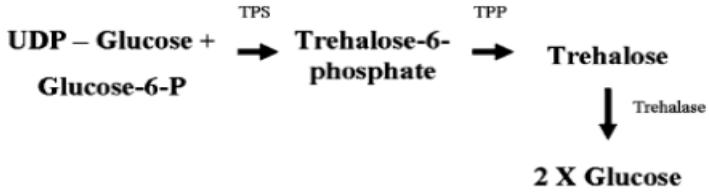

Figure 2: Trehalose's Biosynthetic pathway (adapted from Almeida, et al, 2007)

1.4 Nicotiana tabacum

Nicotiana tabacum (tobacco) has been used as a model plant for decades and is one of the most studied higher plant species.I It belongs to the Solanaceae family and the genus *Nicotiana*, that includes over 60 species. Tobacco plants occur naturally in tropical and temperate regions of every continent however is in Central and South America that reaches the higher expression and diversity.

This species (*Nicotiana tabacum* L.) results of a natural hybridization of two native species, *Nicotiana sylvestris* & *Nicotiana tomentosiformis* approximately 6 million years ago[24].

The original species originates from the borders of mid or lower altitude forests of the Central and Southern America, presented small seeds, sensitive to the light. Tobacco is grown in full sun, in well drained but moisture retentive soils, rich in organic material[24,25].

Tobacco is a large and robust annual plant, with some varieties growing to 3 m in height, and developing a semi-woody stem, in a single growing season. The leaves can get up to 40 cm or more in length. Tobacco flowers are typically tubular and around 5 cm long with a rose-pink color, which are mildly fragrant and borne in hanging clusters in late summer[25].

.

1.5 Proteomic approaches

Proteomics is a relatively new field of research that emerged in the past few decades, and has the objective of characterizing the proteome of an organ or organism, being the science of large-scale analysis of proteins. To do so, proteomics bases itself in two main aspects, protein separation (mainly by gel basis approaches) and identification and characterization of proteins and peptides (mainly Mass Spectrometry (MS) approaches)[26,27]. Both approaches will be discussed further below.

1.5.1 Gel based

Quantitative protein expression analysis is one of the most challenging aspects in proteomics[28].

Two-dimensional polyacrylamide gel electrophoresis (2-DE-PAGE or 2-DE) has been the separation technique, by default, in proteomic studies and it remains one of the key methodologies. In this technique, proteins undergo the first dimension, an isoelectric focusing (IEF), in which, the proteins, are separated by isoelectric point. The second dimension separates the proteins by molecular mass in the presence of denaturating agents. Two-dimensional electrophoresis was first introduced by O'Farrell in 1975. In the original technique, the first dimension separation was performed in carrier-ampholyte-containing polyacrylamide gels cast in narrow tubes [29,30]. In-gel detection of proteins is historically made, preferentially by two methods, Silver or Colloidal Coomassie Blue (CCB) stainings[26]. However these methods have some limitations in terms of sensitivity, dynamic range and reproducibility. Therefore, the detection, may be improved using the differential gel electrophoresis (DIGE) that exploits the higher detection of proteins labeled with fluorescent dyes that can be spectrally resolved and then identifying the proteins by Mass Spectrometry assays [28,31,32].

The key benefit of DIGE is that it allows the incorporation of the same internal standard on every gel in the assay, enabling to produce qualitative and quantitative data. By tagging the samples with different cyanine dyes that provide different fluorescence wavelengths for detection, two differentially labeled samples can be combined and co-separated on the same gel, reducing the amount of gels needed and avoiding the gel to gel variation raises the confidence of the detected differences[28,33] as demonstrated in Figure 3. Fluorescent dye provide a large sensitivity, detecting about 125 pg of protein and providing a linear response to protein concentration of up to four orders of magnitude[27].

After software analysis, gels are ready to be cut, choosing to excise the spots of greatest interest to the subject under study. These will be submitted to an in gel digestion, typically with trypsin, so that the peptides generated can then be analyzed by MS and the protein identification inferred.

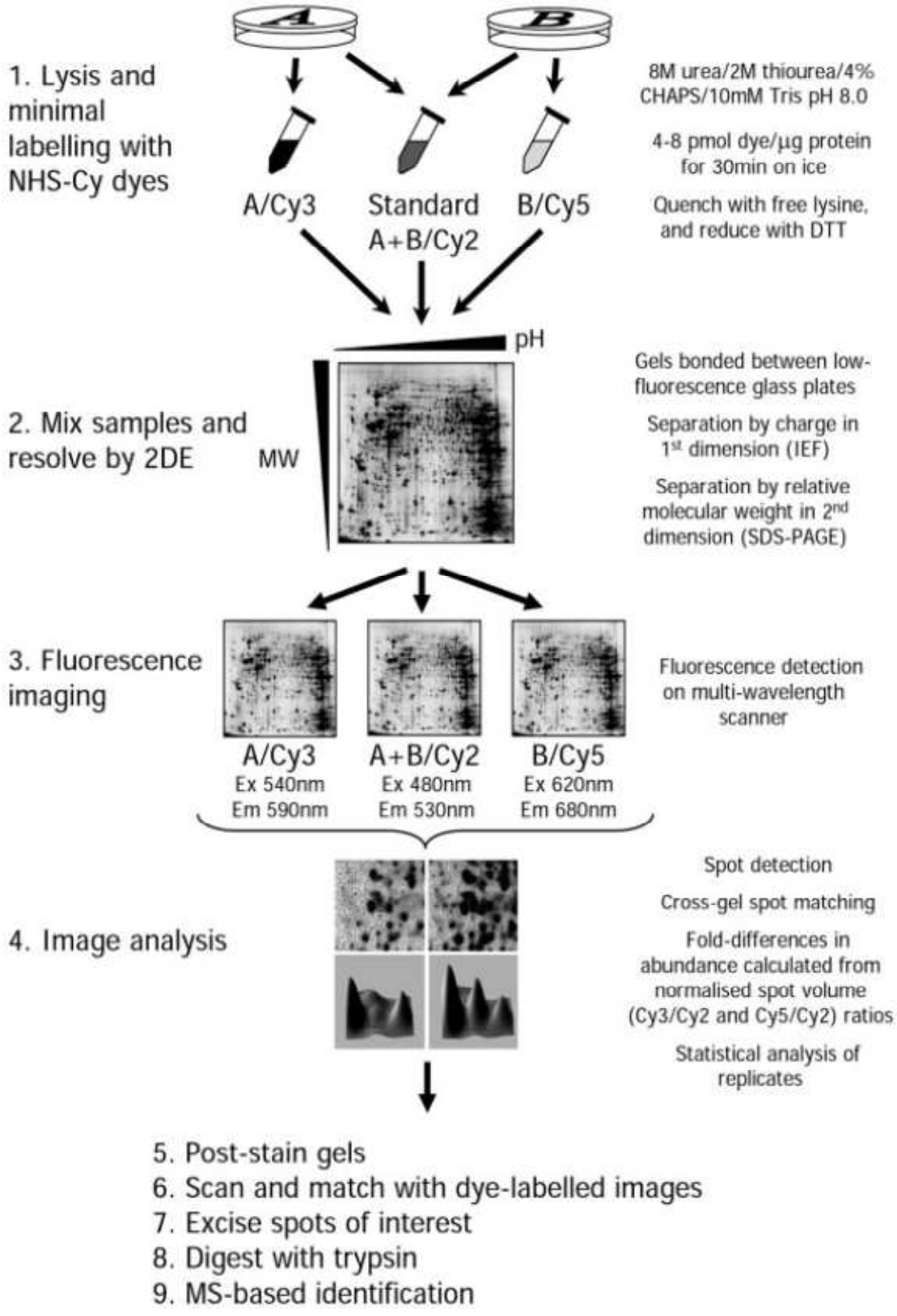

Figure 3: work flow of a DIGE experiment adapted from Timms and Cramer 2008[28]

1.5.2 Mass Spectrometry

MS based proteomics has emerged as a new and potent, technology in the last decade and quickly become a routine in many laboratories, allowing the identification of

proteins present in complex mixtures, often without previous knowledge of its composition[27]. To identify protein it is needed to have good data in the peptide masses in terms of sensitivity and resolution[34]. Mass spectrometry methods measure m/z of ions of compounds with high accuracy and precision. Tandem mass spectrometry (MS/MS) identifies the origins of the fragment ions[35,36].

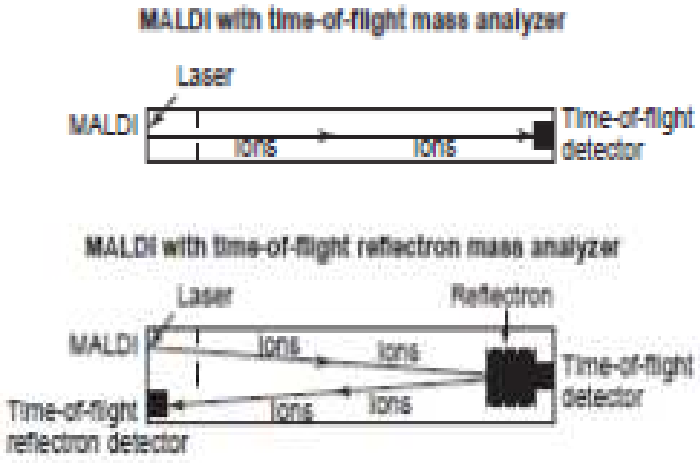

Figure 4 MALDI-TOF and TOF/TOF analyzer squeam, adapted from J. Kathleen Lewis, Jing Wei, and Gary Siuzdak 2000

Protein rapid identification is a task frequently addressed by matrix-assisted laser desorption/ionization time-of-flight mass spectrometry (MALDI/TOF-MS), MALDI results in a nondestructive vaporization and ionization of both large and small biomolecules. It introduces an organic matrix (such as α-cyano-4-hydroxycinnamic acid) in a large molar excess, that co-crystallize with the analyte [36–38]. The matrix absorbs the laser and vaporizes carrying the analyte with it; the matrix also serves as a proton receptor and donor, contributing to ionize the analyte in both negative and positive modes[37]. MALDI ionization source can be used in two types of mass analysers, the Time-of-Flight (TOF) and a TOF reflectron. TOF analysis is the simplest and is based in the time that a set of ions takes to reach the detector after being accelerated, if the ions were submitted to the same amount of energy. As the ions have the same energy but not the same mass, the ions reach the detector at different times[37].

TOF reflectron (TOF/TOF) combines the TOF technology with the reflectron, an electrostatic analyzer, which increases the ions time of flight while reducing their kinetic energy enhancing the resolution of the technique (Figure 4)[37].

1.6 Previous work

1.6.1 Previous works with TPS

In 1997 Goddijn et al. used the OtsA gene from E. coli, successfully transformed both tobacco and potato plants and obtained trehalose accumulation in transgenic tobacco that displayed abnormal phenotypes such as stunted growth and lancet-shaped leaves[39]. Using a construct with the TPS1 gene from S. cerevisae, Romero et al. genetically engineered tobacco whilst Yeo et al. in 2000 made the same with potato plants. Again, abnormal phenotypes such as those described earlier were detected and trehalose accumulation was shown in both cases. Drought tolerance was increased in transgenic plants by comparison with wild type plants.

A fusion gene (TPSP) of both E. coli genes involved in trehalose biosynthesis has been used for the genetic engineering of rice[40,41]. According to Garg et al. 2002, several transgenic lines were established and exhibited sustained plant growth, less photo-oxidative damage under salt, drought and low temperature stress conditions and accumulated trehalose[42]. The same gene construction was also introduced into rice plants under the control of a different promoter by Jang et al., 2003. The trehalose levels increased significantly in leaf and seed extracts of transgenic plants to levels of up to 1.076 mg/g fresh weight, while carbohydrate profiles were similar to wild-type control plants[43]. In 2004, Avonce and coworkers reported that over-expression of Arabidopsis AtTPS1 gene in Arabidopsis that conferred drought tolerance without causing morphological changes[44], and in 2005 Almeida and colleges also using the Arabidopsis AtTPS1 transformed *Nicotiana tabacum*[22] Almeida's work will be further addressed in point 1.6.3.

More recently in 2011 Li et al found that transgenic lines overexpressing OsTPS1 have enhanced tolerance of rice seedling to cold, high salinity and drought treatments without other significant phenotypic changes by increasing the amount of trehalose and proline, and regulating the expression of stress-related genes[45].

1.6.2 Previous Proteomic work in heavy metal stress en plants

In 2001,employing high-resolution two-dimensional electrophoresis (2-DE), Hajduch et al. studied changes in the rice leaf protein patterns, in response to applied heavy and

alkaline metals detecting, severe changes in 2-DE protein patterns after exposure to copper, cadmium, and mercury, over control, including differences in the major leaf photosynthetic protein, ribulose-1,5-bisphosphate carboxylase/oxygenase (RuBisCO, both suppression and fragmentation) suggesting a highly specific action of some of these metals in disturbing the photosynthetic machinery[46]. In 2006, Sarry et al, using 2-DE and LC-ESI-MS, revealed that the main variation at the protein level came from the presence of six different families of phytochelatins, in *A. thaliana* cells treated with Cd[14]. In 2007 Bona and coworkers, investigated copper effects on the root proteome of *Cannabis sativa*, finding that Copper stress induced the suppression of two proteins, the down-regulation of seven proteins, while five proteins were up-regulated. The resulting differences in protein expression pattern were indicative of a plant adaptation to chronic stress[47]. Kieffer et al (2008) used young poplar plants (*Populus sp*.) leaves exposed to Cd, they analysed the protein extracts by 2-DE-DIGE, followed by MALDI-TOF-TOF identification, found that the negative effect of Cd could be explained by a deleterious effect on protein expression from the primary carbon metabolism and from the oxidative stress response mechanism[48]. In 2009 Farinati and colleagues, using *Arabidopsis halleri* grown in heavy metal-contaminated soil and analyzing the proteome by 2-DE followed by MS, found a general up-regulation of photosynthesis-related proteins in plants exposed to metals, and also that proteins involved in plant defense mechanisms were down-regulated indicating that heavy metals accumulation in leaves supplies a protection system and highlights a cross-talk between heavy metal signaling and defense signaling[49]. In 2008 Zhao et al studied the effects of Cd exposure on protein expression patterns of *Phytolacca americana*. They verified several key proteins alterations, involved in distinct metabolic pathways by immuno-blot analysis. Major changes were found for the proteins involved in photosynthetic pathways. One-third of the up-regulated proteins were attributed to transcription, translation and molecular chaperones[50]. These previous works help to understand potential effects heavy metal induced stress in plants, which is important in the present work.

1.6.3 Tobacco strains origin and preliminary works with heavy metal stress

The *Nicotiana tabacum* strains used in the present work had their origin in the work published by Almeida and colleagues in 2005 in which a cassette harboring the AtTPS1

gene under the control of the CaMV35S promoter and the Bialaphos resistance gene was inserted in the binary plasmid vector pGreen0229 and used for *Agrobacterium*-mediated transformation of tobacco, originating three strains, B5A, B5H (both presenting high expression of TPS) and B1F (presenting lower but yet relevant expression of TPS) as confirmed by northern and western blot. Plants presented higher tolerance to drought, osmotic and temperature stresses[22]. In 2007, Almeida and colleagues further analyzed the B5H and B1F strains in terms of the photosynthetic response of these two strains, comparing to a wild type, in response to water withdrawal stress. Their results indicate that the B5H strain possible have a higher ability to withstand severe drought stress and to resist to prolonged periods without water than the B1F and WT lines[21].

In 2009 Batista presented an MSc thesis about the evaluation of the response to oxidative stress induced by cadmium and copper in tobacco plants transformed and Wild type, using the strains B5H and B1F. The plants were grown in hydroponic solution with different concentrations of these metals. Baptista measured the protein content in leaves, in terms of antioxidative enzymes (CAT, POD, SOD, APX), lipid peroxidation and hydrogen peroxide were determined in leaves. The results lead to the conclusion that B1F plants seem to be less affected by oxidative stress induced by Cd and Cu than B5H or WT[51].

1.7 Objectives of the current work

As referred earlier heavy metal contamination is an increasing problem in the modern world. It is essential to start using heavy metal tolerant plants in phytoremediation of contaminated area and grow economically interesting. It is also important to use non-crop plants with enhanced heavy metal tolerance, which may have interest in other non-food applications such as forestry or industrial fiber production for instance.

The previously-mentioned results led to the hypothesis that plant genetic engineering with the trehalose bio-synthesis gene leads to the increase in abiotic stress tolerance, both at the level of water deficit and heavy metal (cadmium) stresses. Such higher tolerance will necessarily have impact at the level of protein expression. The aim of the present work is therefore to study the effects of a Cd exposure of two transgenic *Nicotiana tbacum* lines (B5H and B1F), which had already shown enhanced tolerance

towards heavy metal-induced stress, in comparison to wild type using a proteomics approach. Differentially expressed proteins between control and treated plants are to be identified and their possible roles in Cd stress responses discussed. Using this novel strategy that, to best of our knowledge has never been applied, we will be able to understand, at the biochemical level, which are the proteins implicated in the transgenic plants ability to withstand heavy metal stress as induced by cadmium.

2 Material and methods

Plant material

Plant material used in this work had its origin in the work of Almeida et al. in 2005, where a cassette harboring the AtTPS1 gene under the control of the CaMV35S promoter and the Bialaphos resistance gene was inserted in the binary plasmid vector pGreen0229 and used for *Agrobacterium*-mediated transformation of *Nicotiana tabacum* plants [22]. We chose two of the three original strains which already shown enhanced tolerance to water deficit and osmotic stress (Almeida et al., 2005, 2007) and heavy metal induced-stress in a physiology study by Batista (2009). The strains used were B5H, B1F originated from *Nicotiana tabacum* cv. Petite Havane which wild types were used as controls. Culture conditions have been previously described by Baptista,[51]. Briefly, all strains were gown in hidroponic culture with Hogland's nutritive solution in 2 L capacity boxes. Each of the strains and Wt were grown in conditions of heavy metal contamination Cd (25, 50 and 100 µM), Cu (50, 100 e 200 µM) and As (25, 50 and 100 µM) We used the 50 µM of cadmium concentration and a zero control for each strain, for now on refered to as Wt C (Wild type zero control) Wt Cd 50 (Wild type treated with 50 µM of cadmium), B5H C (B5H zero control), B5H Cd 50 (B5H treated with 50 µM of cadmium), B1F C (B1F zero control) and B1F Cd 50 (B1F treated with 50 µM of cadmium). We choosed cadmium, due to its importance as contaminant and we choose the 50 µM concentration, because it should provide a good insight in the protein patter variation. The last expanded leaf was cut and immediately frozen in liquid Nitrogen and kept at -80ºC until further analysis. All procedures described in this

section were conducted in a preliminary phase of the project and not by the author of this MSc thesis. Information herein described is reported only for descriptive purposes and to present the framework in which the proteomics analysis was later conducted.

Figure 5: Picture of tobacco plants grown under hydroponic conditions. Adapted from Batista[51]

Protein extraction and concentration

The plant material was emerged in N_2 and ground with a Mikro-Dismembrator S (Sartorius, Goettingen, Germany) at 3.000 rpm for 90 seconds. Proteins were precipitated with a solution of 60 mM dithiothreitol (DTT), 10 % trichloroacetic acid (TCA) in Acetone (w/v) cooled at -20ºC and incubated for 1 hour at -20ºC and later vortexed for 15 seconds followed by a 16.000G, 10 minutes centrifugation at 4ºC. The pellet was first washed in 100 mM ammonium acetate in methanol cooled at -20ºC and then in 80 % acetone cooled at -20ºC. Between each wash, the pellet was incubated at -20ºC for 30 min and was afterwards vortexed for 15 seconds, followed by a 16.000G centrifugation at 4ºC and for 10 minutes. The pellets were dried for 1 hour in a Thermomixer (Eppendorf, Hamburg, Germany) at 800 rpm, at room temperature (RT) and were then dissolved in IEF DIGE lysis (buffer 30 mM Tris, 7 M Urea, 2 M Thiourea, 4% (w/v) 3-[(3-Cholamidopropyl) dimethylammonio]-1-propanesulfonate (CHAPS), pH 8.5) for 2-DE gel electrophoresis. Protein quantitation

was performed using the 2D Quant Kit (GE Healthcare, Uppsala, Sweden), following manufacturer's instructions.

2.1 2-DE Optimization

For the first-dimension, 600 µg of protein from each extract were incubated with urea rehydration solution (8 M urea, 2% (w/v) CHAPS, 0.28% (w/v) DTT), 2% IPG buffer 3-10NL (GE Healthcare, Uppsala, Sweden) and a trace quantity of bromophenol blue, to a total volume of 450 µL, for 1 hour at room temperature and were then centrifuged at 16.000 G for five minutes. This solution was used for the active rehydration of 24 cm Immobiline™ DryStrip pH 3-10NL strips (GE Healthcare, Uppsala, Sweden) covered with Immobiline™ DryStrip Cover Fluid (GE Healthcare, Uppsala, Sweden) during 12 hours at 30 V. The active rehydration and the remaining of the IEF setup were run in an Ettan™ IPGphor™ 3. The remaining of the IEF setup was as follows, 1 hour at 200 V, 1 hour at 500 V, 1 hour at 1.000 V, a gradient of 30 minutes set to 8.000 V and a final step at 8.000 V until reaching 50.000Vh.

After IEF, the strips were equilibrated, in order to reduce and alkylate the proteins. Strips were equilibrated in equilibration buffer (6 M urea, 75 mM Tris-HCl pH 8.8, 29.3% (v/v) glycerol, 2% (w/v) SDS, 0.002% (w/v) bromophenol blue) with either 6.5 mM DTT and 10 mM iodoacetamide (IAA) during 15 minutes for each stage of the process.

The second dimension was performed, on large slab, 1 mm thick and 12.5% acrylamide gels (Acrylamide 40% 29:1, 1.5 M TrisCl, pH 8.8, 10% (w/v) SDS, 10% (w/v) Ammonium Persulfate (APS), 10% (v/v) Tetramethylethylenediamine (TEMED)). The second dimension was performed in Ettan™ DALTsix (GE healthcare, Uppsala, Sweden) with Laemmli electrophoresis buffer (25 mM Tris base, 192 mM glycine, 0.1% (w/v) SDS) and the running conditions were 10 mA/gel, 80 V, 1 W/gel during 1 hour followed by 15 W/gel until the dye front reached the end of the gel. Gels were stained with Colloidal Coomassie Blue (see section on visible staining)

RuBisCo depletion trial

The RuBisCo depletion was attempted by adapting a protocol used by Kim and co-workers[52]. The plant material was emerged in N2 and ground with a Mikro-Dismembrator S (Sartorius, Goettingen, Germany) at 3.000 rpm for 90 seconds, and the grinded samples were suspend in 1mL of Mg/tritonx100 solution containing 0.5 M Tris-HCl, pH 8.3, 2% v/v tritonX100, 20 mM MgCl2, 2% v/v β-mercaptoethanol. The extracts were centrifuged at 12.000G for 15min the supernatant was saved and 200 µL of a 50% (w/v) polietilenoglicol (PEG) solution was added to the supernatant and incubated on ice for 30 minutes and then centrifuged at 1.500G for 10 minutes the pellet was saved and 200µL of a 50% PEG solution was added to the supernatant and Incubated on ice, for 30min followed by 15 minutes of centrifugation at 12.000G; the pellet was saved and 80% acetone was added to the supernatant, incubated, on ice for 30 min then centrifuged at 12.000G for 15min. Proteins were precipitated with a solution of 60 mM DTT, 10 % TCA in Acetone (w/v) cooled at -20ºC and incubated for 1 hour at -20ºC, then vortexed for 15 seconds, followed by a centrifugation at 16.000G for 10 minutes at 4ºC. The resulting pellet was first washed in 100 mM ammonium acetate in methanol cooled at -20ºC and then in 80 % acetone cooled at -20ºC. Between each washes, pellet was incubated at -20ºC for 30 min, followed by 15 seconds vortexing and 16.000g, 10 minutes at 4ºC centrifugation. The pellets were dried for 1 hour in a Thermomixer (Eppendorf, Hamburg, Germany) at 800 rpm, at room temperature (RT) and then were dissolved in IEF DIGE lysis buffer (30 mM Tris, 7 M Urea, 2 M Thiourea, 4% (w/v) CHAPS, pH 8.5) for 2-DE gel electrophoresis.

Plant tissue amount and volume of buffer trial

Three different quantities of plant tissue and three different volumes were tested. In terms of plant tissue were accessed 1leaf, 1.5 leaves and two leaves, in terms of lysis buffer volume, 500 µL, 750 µL and 1mL mere accessed. 30 µg of quantified protein were runned in a 1-D gel stained with CCB.

Visible Staining

Visible staining was performed to visualize the spots that would be selected for manual picking upon gel analysis. Coloidal Coomassie Blue (CCB) or Silver staing were respectively used for larger and smaller spots. All gels used in 2-DE protocol optimization were also subjected to Coloidal Coomassie Blue staining.

Silver Staining was performed using the SilverQuest™ Silver Staining Kit (Invitrogen, Carlsbad, California) with several changes being made to the manufacturer protocol. We used 300 mL of each solution per gel; 45 min in sensitizing instead of 10 min; 20 min in 30% ethanol instead of 10 min, 30 min in staining instead of 15 min, and use 30 mL of Stopper instead of 10 mL. The distaining protocol was made following the manufacturer protocol. A total of 100 µL of 50% (v/v) mixture of Distainer A and B was added to the exized spots and incubated at room temperature for 15 minutes, then the solution was removed and ultra pure water was added and incubated also at room temperature for 10 minutes. This step was repeated until the spots were completely distained.

For CCB, gels were stained in a solution of 7.84% (w/v) Ammonium sulphate, 1.57% (v/v) Ortho-phosphoric acid, 0.08% (w/v) Coomassie G-250, 20% (v/v) Methanol)[53] for 48h under agitation followed by five successive steps of washing with double-distilled water for 15 minutes.

2-DE-DIGE

2-DE-DIGE was performed following instructions from the manufacturer (GE Healthcare, Uppsala, Sweden). The pH of each sample was adjusted to 8.5 with 100 mM and 250 mM NaOH solution, using pH test srips (Sigma-Aldrich, St. Louis, Missouri) in the day when labelling would be performed and using 24 cm Immobiline™ DryStrip pH 3-10NL strips (GE Healthcare, Uppsala, Sweden). An internal standard (IS) was made by mixing 30 µg of each of the samples used in the study. The samples (30 µg) and the internal standard were labelled with CyDye DIGE Fluor minimal dyes (240 pmol per 30 µg protein, GE Healthcare, Uppsala, Sweden) and incubated on ice for 30 min in the dark. One microlitter of 10 mM Lysine was then added to stop the reaction, and the samples were left on ice for 10 min in the dark. Replicates were multiplexed randomly and CyDye swap was performed according to the experimental defined, as

present in Table 1 in order to prevent bias results in gel image analysis. As shown in the follwing table this work was divided in two assays, one directly comparing the B5H strain control (B5H C) and treated with 50 µM of cadmium (B5H Cd 50), with Wild typet control (Wt C) and trated with 50 µM of cadmium (Wt Cd 50) refered from mow on as B5H/Wt assay and other one directly comparing the B1F strain control (B1F C) and treated with 50 µM of cadmium (B1F Cd 50), with Wt C and Wt Cd 50, refered from mow on as B1F/Wt assay.

Cy2[1]	Cy5[1]	Cy3[1]	Cy2[2]	Cy5[2]	Cy3[2]
Wt+B5H sample pool	Wt C(1)	B5H C(6)	Wt+B1f sample pool	B1F C(6)	Wt C(1)
	Wt Cd 50 (1)	B5H Cd 50 (6)		B1F Cd 50 (6)	Wt Cd 50 (1)
	B5H Cd 50 (5)	Wt C(2)		Wt C(2)	B1F Cd 50 (5)
	B5H C(5)	Wt Cd 50 (2)		Wt Cd 50 (2)	B1F C(5)
	Wt C(3)	B5H Cd 50 (4)		B1F C(4)	Wt C(3)
	Wt Cd 50 (3)	B5H Cd 50 (4)		B1F Cd 50 (4)	Wt Cd(3)
	B5H Cd 50 (3)	Wt C(4)		Wt C(4)	B1F Cd 50 (3)
	B5H C(3)	Wt Cd 50 (4)		Wt Cd 50 (4)	B1F C(3)
	Wt C(5)	B5H C(2)		B1F C(2)	Wt C(5)
	Wt Cd 50 (5)	B5H Cd 50 (2)		B1F Cd 50 (2)	Wt Cd 50 (5)
	B5H Cd 50 (1)	Wt C(6)		Wt C(6)	B1F Cd 50 (1)
	B5H C(1)	Wt Cd 50 (6)		Wt Cd 50 (6)	B1F C(1)

Table 1: sample randomization for DIGE assays: [1] represent the B5H/Wt assay and [2:] the B1F/Wt assay in the first line is represented which Cy Dye is to be used in each column

The two samples (30 µg) for each batch and the internal standard (30 µg) were mixed before adding 2x lysis buffer (7 M urea, 2 M thiourea, 4% CHAPS (w/v), DeStreak Reagent (GE Healthcare, Uppsala, Sweden)) to a final volume of 450 µl, and 2% v/v ampholytes immobilized pH gradient (IPG) buffer (pH 3-10, GE Healthcare, Uppsala, Sweden) (see Table 2 and 3 for further details). The batch was left on ice for 10 min in the dark before loading onto IPG strips (Immobiline Dry Strips, 24 cm, pH 3-10 NL, GE Healthcare, Uppsala, Sweden) for isoelectric foccusing. The current experiment thus contained six biological replicates.

Table 2: table containing the mixtures made for each IPG strip in the B5H/Wt assay

B5H/Wt	Cy5[1]	V(µL)[2]	Cy3[3]	V(µL)[4]	pool Cy2 V(µL)[5]	samples total (µL)[6]	2xLysis[7]	deStreak[8]	Total[9]
1	wtc1	13,77	B5HC6	11,35	16,13	41,24	41,24	367,52	450,00
2	WtCd50_1	17,79	B5HCd50_6	16,34		50,26	50,26	349,47	450,00
3	B5HCd50_5	18,39	wtc2	15,00		49,52	49,52	350,96	450,00
4	B5HC5	17,24	WtCd50_2	14,89		48,26	48,26	353,49	450,00
5	wtc3	20,16	B5HC4	15,98		52,26	52,26	345,49	450,00
6	WtCd50_3	17,24	B5HCd50_4	14,48		47,85	47,85	354,31	450,00
7	B5HCd50_3	10,73	wtc4	14,40		41,26	41,26	367,48	450,00
8	B5HC3	12,90	WtCd50_4	29,41		58,44	58,44	333,13	450,00
9	wtc5	19,57	B5HC2	10,93		46,63	46,63	356,75	450,00
10	WtCd50_5	19,45	B5HCd50_2	14,50		50,07	50,07	349,85	450,00
11	B5HCd50_1	9,10	wtc6	12,50		37,73	37,73	374,54	450,00
12	B5HC1	14,85	WtCd50_6	26,07		57,05	57,05	335,90	450,00

Table 2: [1]samples marked with Cy5; [2]volume of the sample for 30 µg of protein; [3]samples marker with Cy3; [4] volume of sample containing 30 of protein. [5] contains the volume of sample pool B5H/Wt marked with Cy2 for 30 µg. The [6]column contains the total volumes of the samples marked with Cy5 and Cy3 and sample pool. [7] Contains the volume of 2x Lysis buffer needed to dilute the samples according to the users' manual. [8] contains the volumes of DeStreak solution needed to make 450 µL in the [9] represent the total volume loaded in to each IPG strip.

Table 3: table containing the mixtures made for each IPG strip in the B1F/Wt assay

B1F/Wt	Cy31	V(µL)2	Cy53	V(µL)4	pool Cy2 V(µL)5	samples total (µL)6	2xLysis 7	deStreak 8	Total9
1	wtc1	13,77	B1fC6	22,94	20,31	57,02	57,02	335,95	450,00
2	WtCd50_1	17,79	B1fCd50_6	19,56		57,67	57,67	334,67	450,00
3	B1fCd50_5	17,20	wtc2	15,00		52,51	52,51	344,98	450,00
4	B1fC5	14,92	WtCd50_2	14,89		50,13	50,13	349,74	450,00
5	wtc3	20,16	B1fC4	28,42		68,88	68,88	312,23	450,00
6	WtCd50_3	17,24	B1fCd50_4	29,60		67,15	67,15	315,70	450,00
7	B1fCd50_3	17,25	wtc4	14,40		51,97	51,97	346,07	450,00
8	B1fC3	29,19	WtCd50_4	29,41		78,91	78,91	292,19	450,00
9	wtc5	19,57	B1fC2	30,14		70,03	70,03	309,93	450,00
10	WtCd50_5	19,45	B1fCd50_2	22,42		62,18	62,18	325,64	450,00
11	B1fCd50_1	23,97	wtc6	12,50		56,79	56,79	336,42	450,00
12	B1fC1	11,70	WtCd50_6	26,07		58,09	58,09	333,82	450,00

Table 3: [1]samples marked with Cy3; [2]volume of the sample for 30 µg of protein; [3]samples marker with Cy5; [4] volume of sample containing 30 of protein. [5] contains the volume of sample pool B5H/Wt marked with Cy2 for 30 µg. The [6]column contains the total volumes of the samples marked with Cy5 and Cy3 and sample pool. [7] contains the volume of 2x Lysis buffer needed to dilute the samples according to the users' manual. [8] contains the volumes of DeStreak solution needed to make 450 µL in the [9] represent the total volume loaded in to each IPG strip.

Protein extracts were then loaded on each strip holder and the strips where then placed and covered with Dry Strip Cover Fluid. The active rehydration of the strips and Isoelectric focusing (IEF) were carried out on an Ettan IPGphor 3 system (GE Healthcare, Uppsala, Sweden) using the following programs: rehydration: 30V (step and hold) for 22h, after rehydration the paperwiks where placed and the IEF started according to the program: 150 V (step and hold) for 4h, 300 V (step and hold) for 3h,

1.000 V (gradient) for 6h, 10.000 V (gradient) for 2 h and 10.000 V (step and hold) for 80.000 Vh.

After IEF, the proteins were reduced and alkylated by equilibration of the strips for 15 min in equilibration buffer (50mM Tris-HCl pH 8.8, 6 M urea, 30 % glycerol (v/v), 2 % SDS (w/v), 0.002 % bromophenol blue (w/v)) containing 6.5 mM DTT followed by 15 min in equilibration buffer containing 10 mM iodacetamide. Separation of the second dimension was performed on 1.0 mm thick gels under low fluorescence glass plates (GE Healthcare, Uppsala, Sweden). IPG strips were loaded on SDS-PAGE 12.5 % acrylamide gels and sealed with a 0.5% (w/v) agarose solution. For the second dimension an Ettan DALTsix electrophoresis unit (GE Healthcare, Uppsala, Sweden) was used with electrophoresis buffer (Tris 25 mM, glycine 192 mM, 0.2 % SDS (w/v)). Gels were run at 20 ºC, 1 W/gel for 17H and 17 W/gel until dye front reached the end of the gel.

Gel image acquisition and analysis

Visible stained gels were scanned at 300-dpi resolution using a calibrated densitometer, ImageScanner (Amersham Biosciences, Piscataway, New Jersey), using LabScan version 5.0.

The DIGE images were scanned with a laser-based scanner FLA-5100 (FujiFilm) using 532 and 635 nm excitation lasers (DGR1double filter) for Cy3 and Cy5, respectively, and a 473 nm excitation laser (LPB filter) for Cy2 under Image Reader FLA 5000 version 1.0 (FujiFilm). The 2-DE gels were scanned in low-fluorescence glassplates at a resolution of 100 µm.

The gel images were then analyzed using Progenesis SameSpots analysis software version 3.3.1 from NonLinear Dynamics following the instructions manual. All analytical gels were aligned to its internal standard (IS) and the IS of each gel was aligned to a IS reference gel (chosen by the user). Following detection and filtering of spots, images were separated into groups (Wt C, Wt Cd 50, B1F C, B1F Cd 50, B5H C and B5H Cd 50) and analyzed to determine significant changes in 2-D spot abundance. A hit list of protein species that changed in abundance was generated. An Anova score

was included for each spot and any proteins with an Anova p-value < 0.05 or an absolute abundance variation of less than 1.5 fold were excluded from further consideration.

In- gel Digestion and Mass spectrometry analysis

Spots of interest were excised manualy, using a 1 mL micropete tip with the cutted end. These procedures have been thoroughly described by Ventosa. Briefly, excised gel spots were washed with 50 % (v/v) acetonitrile (ACN) to remove stain traces, then were dehydrated with 100 µL of ACN for 15 minutes, then the ACN was discarded and the spots were incubated in 50 µL of a 10 mM of DTT in 100mM of NH_4HCO_3 solucion for 45 minutes at 56ºC, in order to reduce disulphide bridges, the solution was discarded and the spots were incubated in 55 mM of IAA in 100mM of NH_4HCO_3 solucion for 30 minutes at RT in the dark in order to alkylate the previously reduced disulphide bridges. The spots were then dehydrated with ACN and vacuum-drying. In-gel digestions were performed by adding 20 µL 6.7 ng/µL modified porcine trypsin (Promega, Madison, Wisconsin) in 50 mM NH_4CO_3. The gel pieces absorbed the trypsin solution for 30 min on ice and remaining liquid was removed. Finally 30 µL of 50 mM NH_4CO_3 were added and the samples incubated at 37 °C for 16 h. The obtained supernatant was recovered and gel pieces were further incubated with 200 µL ACN for 15 min then the liquid was recovered. To the gel pieces was added 200 µL of 5 % (v/v) formic acid for 15 min, the liquid was then colected and to the gel pieces was added 200 µL of ACN incubated for 15 min and the liquid was then colected in order to further extract peptides trapped in the gel. Peptides were desalted and concentrated according to the method of Gobom et al.[38] Using homemade zip-tip columns (GELoader tip 0.5-20 µL, Eppendorf, Hamburg, Germany) with Empore™ Octadecyl C18 extraction disks (Supelco Analytical, Sigma-Aldrich St. Louis, Missouri). The column was washed with 20 µL 5 % (v/v) Formic Acid (FA). The tryptic peptides was loaded on the column and afterwards bound peptides were eluted with 0.6 µL of matrix solution (α-cyano-4-hydrocynnamic acid 5 gL^{-1} in 50 % acetronitrile, 5% FA) directly on the MALDI target. Peptide mass spectra were acquired by Applied Biosystems 4800 Plus MALDI

TOF-TOF Analyzer apparatus. Data were acquired in positive MS reflector using PepMix1 calibration mixture (LaserBio Labs, France) standard to calibrate the instrument. Each reflector MS spectrum was collected in a result-independent acquisition mode, typically using eight thousand laser shots per spectra in an 800−4.000 m/z range and a fixed laser intensity of 3.000V. Fifteen of the strongest precursors were selected for MS/MS, the strongest precursors being fragmented first. MS/MS analyses were performed using CID (Collision Induced Dissociation) assisted with air, with a collision energy of 1 kV and a gas pressure of 1 x 10^6 torr[54].

Identification of proteins differentially expressed

Raw data was generated by the 4000 Series Explorer Software v3.5.3 (build 1017) (Applied Biosystems) and contaminant m/z peaks resulting from trypsin autodigestion were excluded when generating the peptide mass list used for data-base search.

Using the mass list, database queries were performed against five databases, UniRef100 2012, NCBInr (20120701), SwissProt 2012, SwissProt 2012 restricted to Viridiplantae (Green Plants), and Medicago (MT_3.5_nt CDSSeq_20100825) using Mascot search engine (version 2.2.04).nd had defined a peptide tolerance of 50 ppm and a MS/MS tolerance of 0.3 Da. The queries had also defined carbamidomethyl of the cysteines as a fixed modification; oxidation of methionines and deamidation as variable modifications. Tryptic peptides with tolerance to one missed cleavage were considered. Depending on the data base protein identification considered valid were the ones with a score of at least 85 (NCBInr and UniRef100); 70 (SwissProt); 67 (Medicago) and 58 (SwissProt 2012 restricted to Viridiplantae (Green Plants)). Mascot search engine calculated the significance ($p < 0{,}05$) for the database used.

It was also used the Protein Pilot software version 3.0, revision 114732; (Applied Biosystems, USA) searches were performed using the NCBInr 20120701 database without taxonomic restrictions and search parameters set as follows: enzyme, trypsin; Cys alkylation, iodoacetamide; special factor, gel-based ID; and ID focus, biological

modification and amino acid substitution. protein identification considered valid were the ones with a score of at least 85[55].

3 Results

3.1 Optimization of 2-DE electrophoresis

For the optimization of 2-DE electrophoresis trials, we used 600 µg of quantified protein extract. We followed the protocol presented previously and Colloidal Coomassie Blue (CCB) staining, to estimate the efficiency of the extraction protocol and the condition of the sample in terms of degradation as well as obtain familiarization with the 2-DE technique.

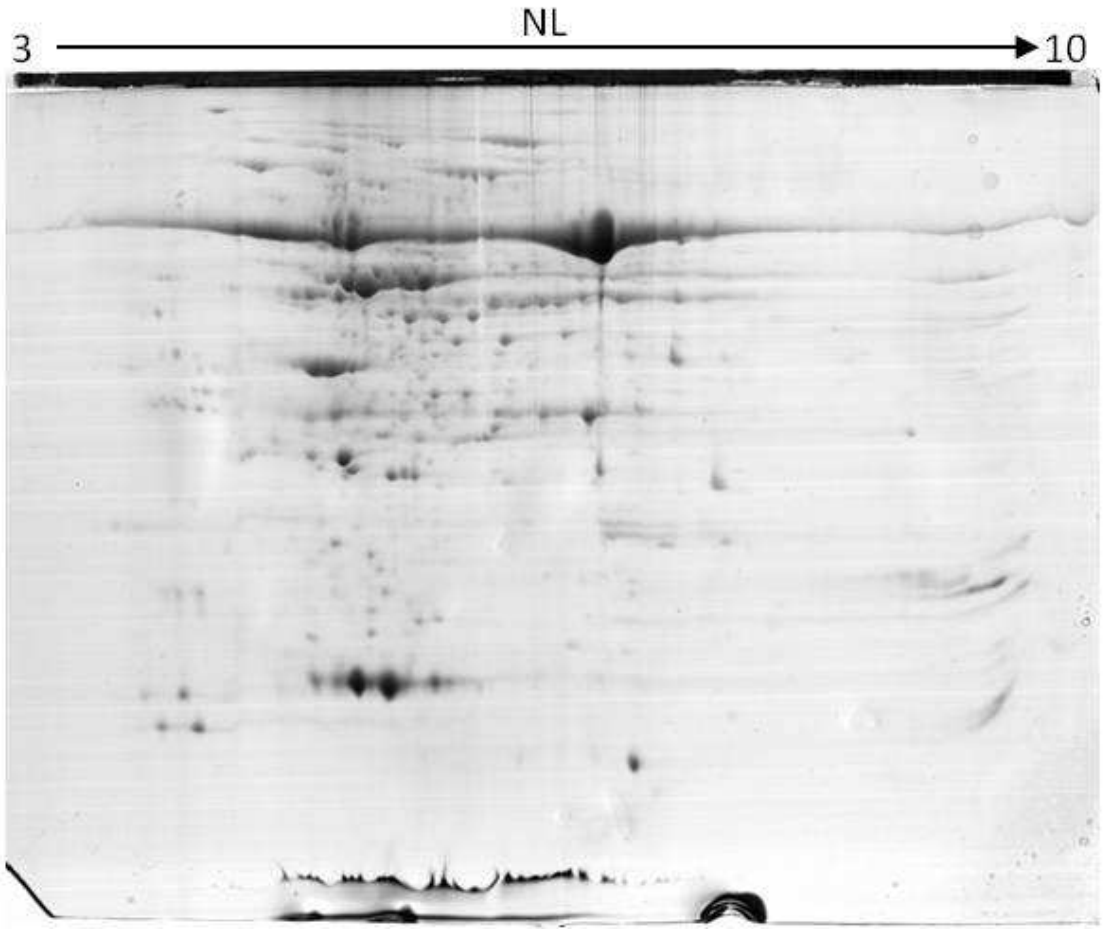

Figure 6: 2-DE gel obtained from 600 µg of protein and CCB stained

Observing the obtained gel image present in figure 6, we noticed a spot belonging to one major protein, RuBisCO which could be masking numerous minor proteins, so we considered performing a RuBisCO depletion protocol.

We used a PEG fractionation protocol, and we performed the 2-DE assay to assess the efficiency of the depletion. We loaded a total of 300 µg of quantified protein extract, that upon 2-DE was stained with Colloidal Coomassie Blue, resulting in the gel images presented in figure 7.

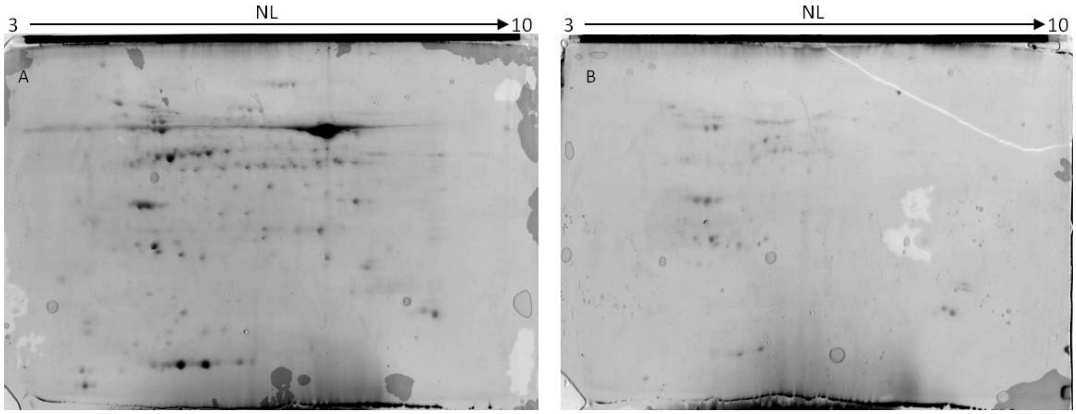

Figure 7: 2-DE gel obtained from 300 µg of protein CCB stained; A: non-depleted sample; B: depleted sample

As may be seen from figure 7, the depletion led to a generalized loss of protein content, not only RuBisCO. As a consequence, and also because in similar studies, leaf protein extracts are rarely depleted, we decided not to conduct the depletion protocol.

An additional optimization question needing to be answered lay in the amount of plant tissue needed to be ground. Accordingly, we have tried several quantities of plant material and volumes of lysis buffer to solubilise the proteins, as seen in figure 8, reaching the conclusion that the equivalent to 1 leaf of plant material was to be ground and proteins solubilised in 500 µL of buffer.

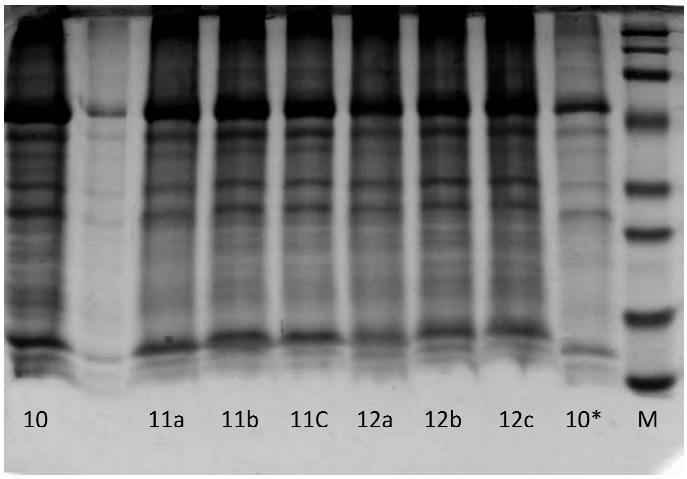

Figure 8: 1D gel, CCB stained containing 30µg of protein in each sample 10: one leaf (500 µL) 10* additional centrifuge step; 11: two leaves; a: 500 µL; b: 750 µL; c: 1 mL; 12: 1.5 leaves; a: 500 µL; b: 750 µL; c: 1 mL

The 1-D gels are simply qualitative due to the interfering of urea present in the buffer

3.2 2-DE-DIGE

As previously explained, all work was divided in two specific assays, one comparing directly B5H to Wild type plants in both 50 µM cadmium exposure and control conditions (B5H/Wt assay) and other comparing directly B1F plants to Wild type plants in both 50 µM cadmium exposure and control conditions (B1F/Wt assay)

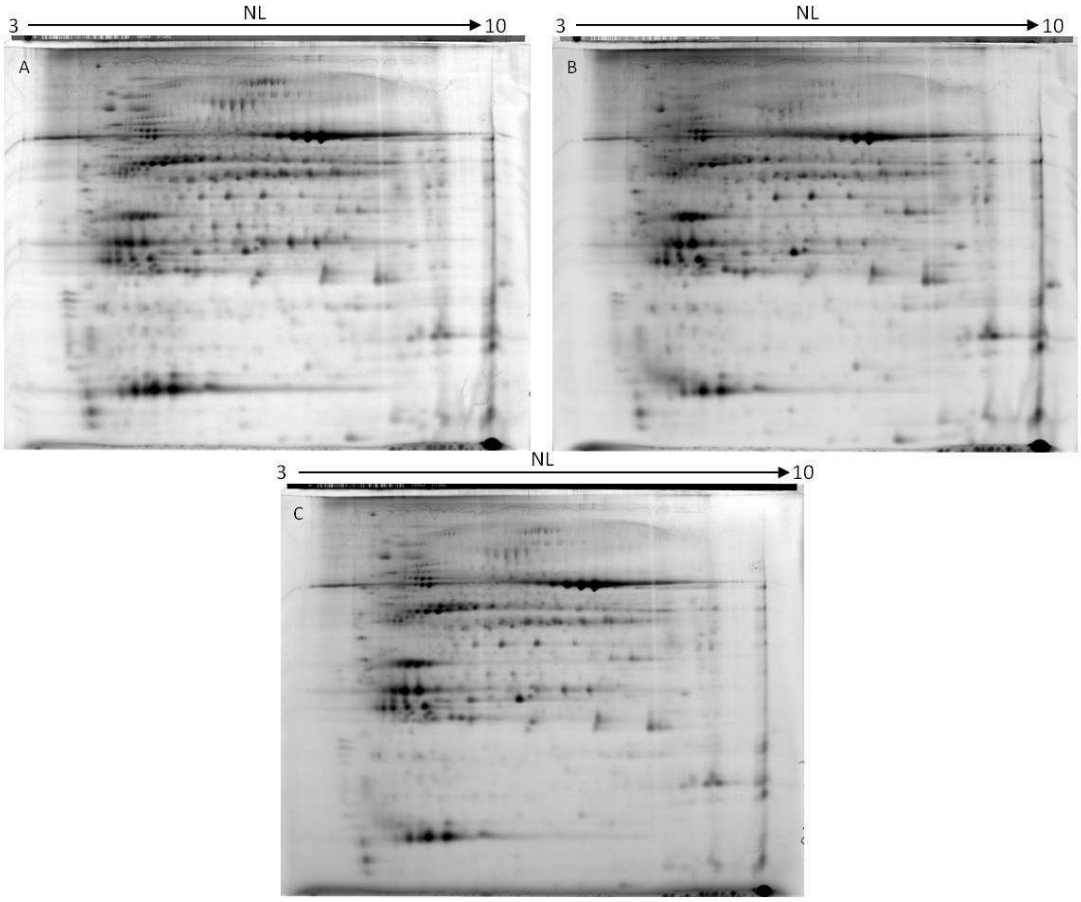

Figure 9: images resulting from one DIGE gel from the B5H/Wt assay; A: Wt treated with 50 µM of cadmium marked with Cy 3 dye; B: B5H control sample marked with Cy 5 dye; C: internal standard marked with Cy2 dye.

Twenty four 2-DE-DIGE runs were made for this work divided in two batches of twelve runs each, according to tables 2 and 3 previously presented. Each gel resulted in three gel images, one for each Cye Dye as shown in figures 9 and 10 for the B5H/Wt and B1F/Wt assay respectively.

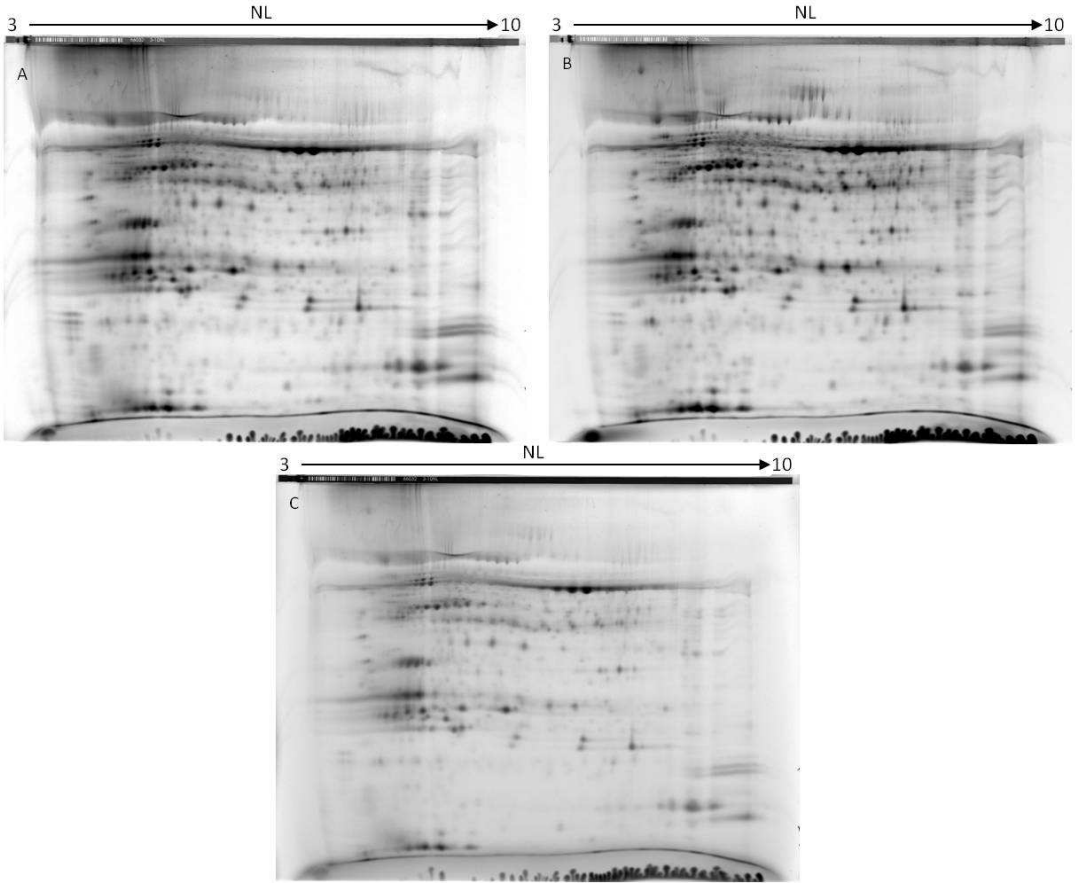

Figure 10: images resulting from one DIGE gel from the B5H/Wt assay; A: B1F control sample marked with Cy 3 Dye; B: Wt treated with 50 µM of cadmium marked with Cy 5 Dye; C: internal standard marked with Cy2 Dye.

Once all the images regarding the two assays were acquired, image analysis was performed.

3.3 Gel image analysis

3.3.1 B5H/Wt assay

Gel analysis using the Progenesis SameSpots for the B5H/Wt resulted in the spot picking image presented in figure 11, as a guide line to excise the spots for MS analysis.

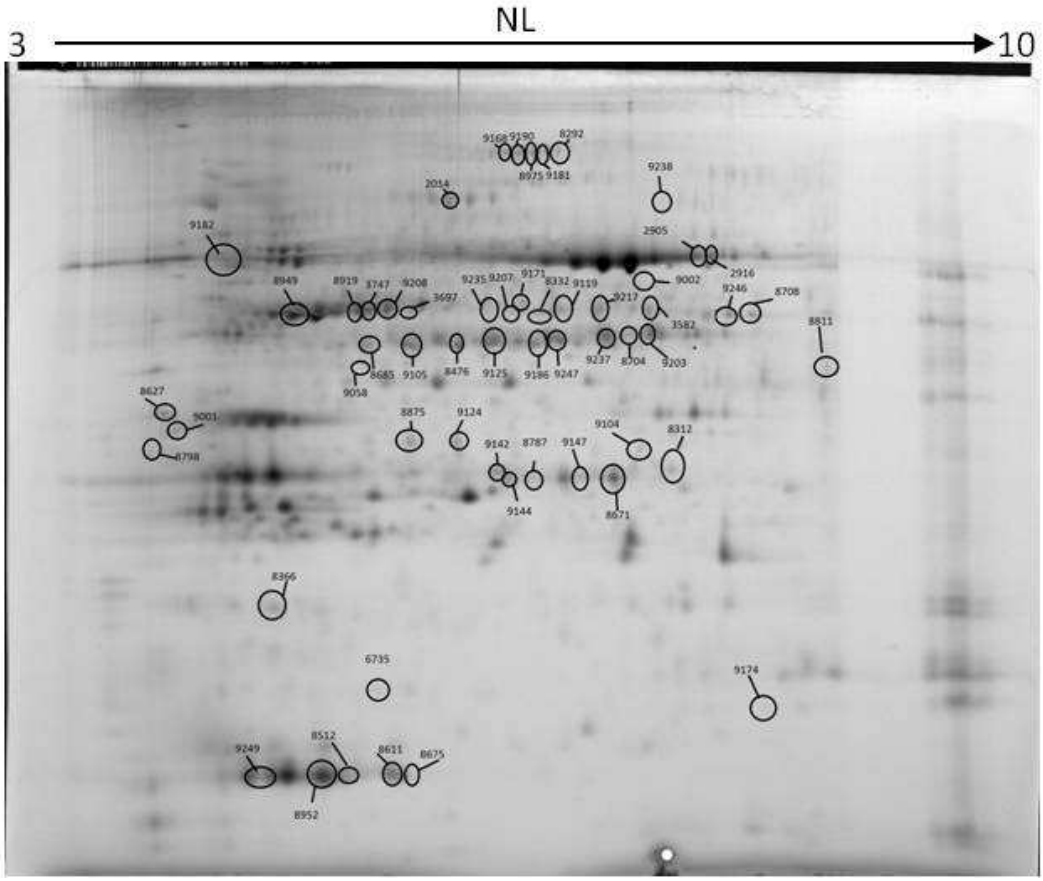

Figure 11: spot picking image resulting from the gel image analysis of the B5H/Wt assay

Progenesis Same Spots gel analysis also created the Principal Component Analysis (PCA), presented in Figure 12. As may be seen, groups Wt C, B5H C and B5H Cd 50 clustered together whereas the group Wt Cd 50 forms a separate cluster.

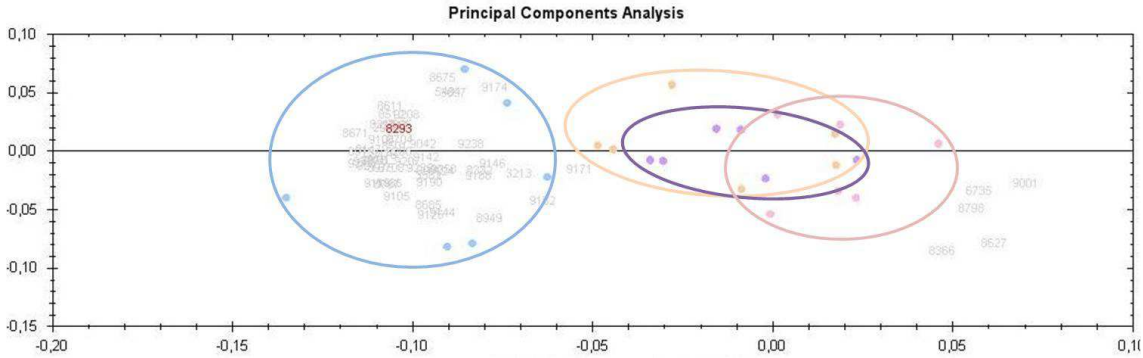

Figure 12: Principal Components Analysis from the assay B5H/Wt representing the four groups in this assay WtC; WtCd50; B5H C and B5H Cd50

From the gel analysis, a list of spots showing differential expression was generated. Results are summarized in Table 4. They indicate that the Average Normalized Volumes, as well as the significance level and the fold for each spot in the four experimental groups.

Table 4: spot list for B5H/Wt assay

#	Anova (p)	Fold	Average Normalized Volumes			
			WtC	WtCd50	B5H C	B5H Cd50
8293	2,84E-06	4,4	0,731	3,202	1,021	1,051
8875	3,51E-06	4,2	0,672	2,847	1,017	1,104
9206	1,44E-05	2,8	0,888	2,513	1,155	1,156
9235	1,70E-05	2,6	0,921	2,394	1,048	1,183
8476	1,73E-05	2,9	0,917	2,651	1,443	1,279
8919	3,00E-05	3	0,812	2,444	1,167	1,299
8787	3,07E-05	3,6	0,765	2,721	1,016	1,103
8671	3,40E-05	7,2	0,696	5,025	1,089	1,608
9119	7,21E-05	3,8	0,866	3,265	0,991	1,445
9247	7,52E-05	3,3	0,922	2,998	1,241	1,214
9181	9,15E-05	3,7	0,782	2,924	1,007	1,118
8512	9,25E-05	2,4	0,985	2,348	1,309	1,437
9105	1,04E-04	2,6	0,852	2,213	1,327	1,169
8312	1,58E-04	3,2	0,89	2,858	1,191	1,224
9147	1,79E-04	3,2	0,964	3,121	1,136	1,415
9238	3,35E-04	2,4	1,013	2,21	0,907	1,034
8708	4,33E-04	2,7	1,031	2,767	1,168	1,45
8685	4,43E-04	3,2	0,758	2,458	1,29	1,087
9104	4,47E-04	2	0,922	1,873	1,102	1,215
9144	5,31E-04	4,5	0,63	2,835	0,926	0,84
8611	8,47E-04	2,1	0,972	2,058	1,335	1,375
9124	0,001	2,8	0,853	2,368	1,055	1,026
2916	0,002	3	0,977	2,957	1,458	1,669
9142	0,002	2,3	1,13	2,574	1,283	1,312
8675	0,003	2,3	0,81	1,834	1,143	1,149
5484	0,003	3,9	0,744	2,902	1,371	1,73
9001	0,004	1,5	1,502	1,003	1,449	1,217
8704	0,004	2,3	1,22	2,769	1,289	1,536
8501	0,004	2,9	1,303	3,763	1,46	1,75
9002	0,004	1,8	1,278	2,037	1,155	1,198
9171	0,005	1,8	0,92	1,626	1,035	1,104
9042	0,005	2,7	1,099	2,938	1,362	1,107
3697	0,005	3,2	0,862	2,747	1,325	1,429
8627	0,005	1,7	1,712	1,02	1,312	1,137
8798	0,005	1,5	1,54	1,001	1,227	1,209
9174	0,006	2,1	0,672	1,387	0,893	0,908

6735	0,006	2	1,187	0,742	0,599	0,972
9182	0,006	1,8	0,852	1,509	1,246	0,981
9058	0,007	1,6	1,247	1,914	1,222	1,196
8949	0,008	2,3	0,762	1,742	1,107	1,004

ANOVA, fold and average normalized volumes calculated, obtained in the image analysis in the B5H/Wt assay

Each spot have a group of four images of the spot in four gel images, one for each experimental group. An example of a graphic ilustrating the results from the expression analysis for two spots (8300 and 9237), is shown in Figure 13. In the annex, individual expression profiles for the differentially expressed proteins that were identified are also represented.

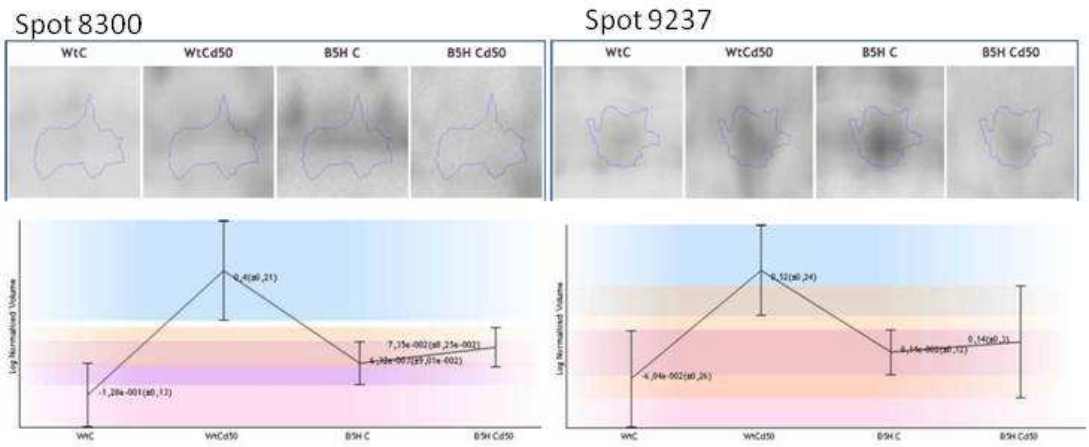

Figure 13: Examples of two spots showing differential expression as a consequence of Cd exposure in the B5H/Wt experiment

3.3.2 B1F/Wt assay

Similar to the previously described the for B5H/Wt image analysis, a Progenesis SameSpots analysis was equally conducted the for B1F and Wt lines, creating the spot picking image presented in Figure 14,

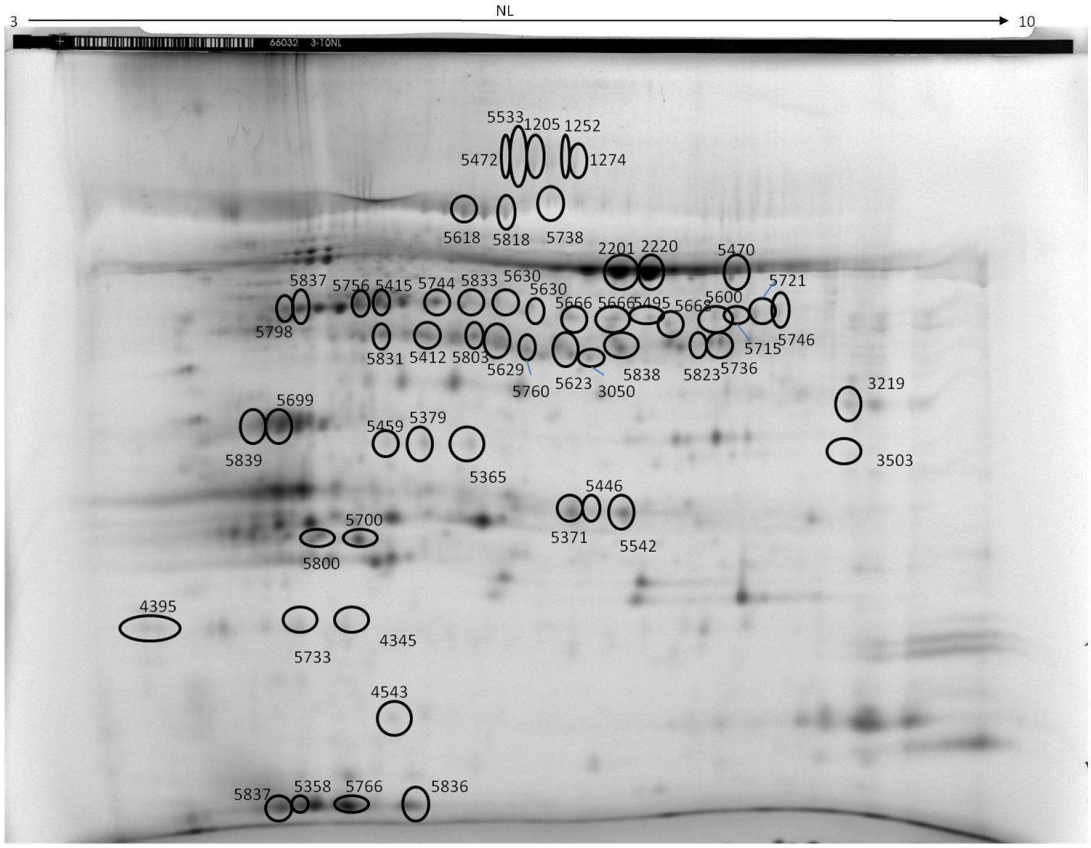

Figure 14: spot picking image resulting from the gel image analysis of the B1F/Wt assay

A Principal Component Analysis (PCA) was also generated and is presented in Figure 15. In this experiment groups Wt Cd 50 and the B1F C clustered separately whereas groups Wt C and B1F Cd 50 seem to have clustered together.

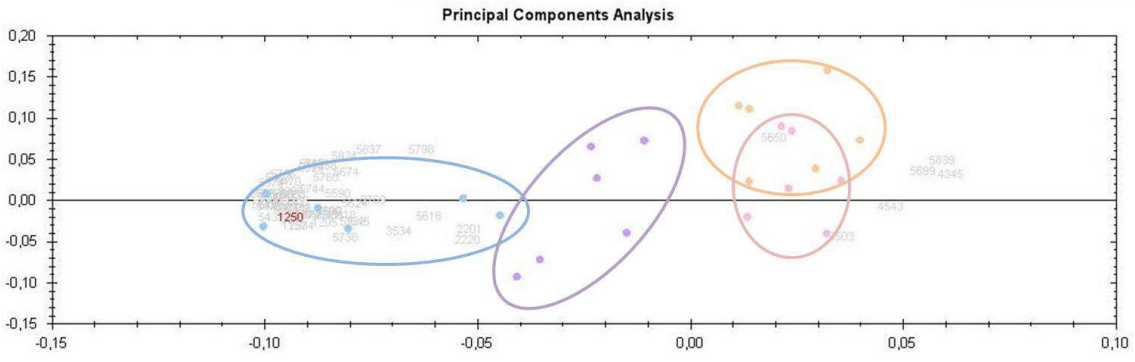

Figure 15: Principal Components Analysis from the assay B1F/Wt representing the four experimental groups for these assay WtC; WtCd50; B1F C and B1F Cd50

A list of the spots presented in the Spot picking image with their anova, fold and average normalized volumes of the spots differentially expressed for this assay is presented in table 2.

Table 5: Spot list for B1F/Wt assay

#	Anova (p)	Fold	Average Normalised Volumes			
			Wt C	Wt Cd 50	B1f C	B1f Cd 50
5832	3,08E-08	2,7	0,893	2,331	1,226	0,873
5473	9,73E-08	2,9	0,842	2,337	1,158	0,82
5495	1,02E-07	3,5	0,828	2,741	1,278	0,788
5625	1,14E-07	3,2	0,732	2,335	1,367	0,855
5666	1,70E-07	4,3	0,623	2,7	1,363	0,722
5838	1,76E-07	3	0,891	2,487	1,268	0,84
5574	2,07E-07	2,8	0,773	2,131	1,386	0,926
5519	2,69E-07	3,1	0,771	2,377	1,172	0,776
5731	2,82E-07	2,9	0,821	2,368	1,192	0,898
5371	4,79E-07	4,2	0,749	2,801	1,264	0,667
5459	6,08E-07	2,6	0,854	2,198	1,152	0,888
5358	6,78E-07	3,4	0,637	2,148	1,446	1,056
5472	8,09E-07	3,7	0,671	2,466	1,217	0,757
5756	9,39E-07	2,4	0,806	1,919	1,382	0,986
1250	1,06E-06	3,9	0,779	2,733	1,228	0,7
1258	1,77E-06	4,5	0,72	2,697	1,219	0,596
5415	2,69E-06	2,8	0,843	2,342	1,537	0,896
5803	3,58E-06	2,2	0,909	2,02	1,306	1,123
5668	5,82E-06	2,4	1,027	2,161	1,507	0,903
5365	7,95E-06	3,4	0,668	2,283	1,175	0,871
5379	8,55E-06	2,3	0,984	2,148	1,104	0,925
5834	9,23E-06	2,3	0,786	1,835	1,261	1,138
5542	1,17E-05	5,3	0,659	3,492	1,206	0,707
5715	1,29E-05	2,8	0,828	2,347	1,204	0,907
1274	1,45E-05	3,5	0,738	2,161	1,32	0,617
5446	1,69E-05	3,1	0,799	2,345	1,257	0,768
5470	2,34E-05	2,7	0,861	2,328	1,395	0,987
5630	2,50E-05	2,9	0,84	2,473	1,26	0,866
1205	3,09E-05	3,1	0,754	2,334	0,94	0,819
5831	3,66E-05	2,1	0,913	1,922	1,404	1,157
3503	3,87E-05	1,7	1,358	0,833	0,831	0,81
5590	4,02E-05	1,9	1,17	1,974	1,329	1,015
5600	4,66E-05	2,5	1,034	1,932	1,261	0,776
5624	5,28E-05	2,7	0,858	2,144	0,922	0,784
5533	7,29E-05	3,9	1,002	2,933	1,301	0,749
5412	7,94E-05	1,9	0,977	1,902	1,377	1,192
5837	1,00E-04	2,4	0,764	1,861	1,425	1,228
5736	1,37E-04	2,4	1,137	2,01	1,34	0,837

3050	1,65E-04	2,1	0,962	2,051	1,239	1,03
5629	1,68E-04	2	0,969	1,975	1,332	1,092
5738	2,58E-04	2,8	0,981	1,958	1,205	0,707
5746	3,87E-04	2,6	0,854	2,221	1,086	0,898
5664	3,99E-04	2,7	1,024	2,106	1,226	0,794
5818	4,12E-04	2	0,926	1,838	1,255	0,945
5798	4,36E-04	2,3	0,791	1,808	1,314	1,266
5674	0,001	2	0,991	1,965	1,129	1,079
3545	0,001	2,5	0,857	1,782	1,193	0,727
5744	0,002	1,9	0,968	1,854	1,388	0,997
5618	0,002	1,8	1,092	1,573	1,149	0,894
5760	0,002	1,8	1,081	1,901	1,286	1,141
5751	0,003	3	1,062	2,442	1,207	0,818
4543	0,004	1,8	1,42	0,863	0,769	1,146
2220	0,005	260,2	0,36	2,907	88,483	0,34
2201	0,006	87	0,582	50,66	43,476	0,622
5699	0,007	1,9	1,852	0,976	1,271	1,415
5839	0,007	1,8	1,679	0,919	1,095	1,458
5650	0,007	1,8	0,891	0,911	1,122	1,609
4345	0,011	1,5	1,24	0,861	1,098	1,294
5769	0,013	2,5	0,98	2,29	1,331	0,905
3534	0,014	2,2	0,823	1,598	0,862	0,714

ANOVA, fold and average normalized volumes calculated, obtained in the image analysis in the B1F/Wt assay

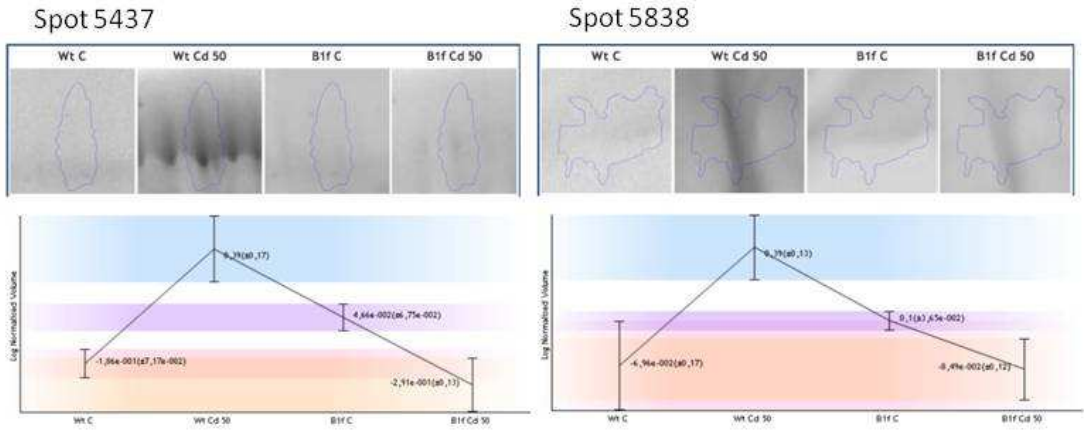

Figure 16: some of the spots identified as differentially expressed in the assay B1F/Wt

Similarly to the previously mentioned experiments, examples of graphics and images, illustrating the variation of spot expression in the four experimental groups of the assay is presented in figure 16. In the annex, individual expression profiles for the differentially expressed proteins that were identified are represented.

3.4 Identification of differentially expressed proteins

After silver or CCB gel staining, a combination was made of the same spot excised from three different gels, in order to maximize the probability of obtaining sound identifications. The use of several databases also increased the probability of obtaining a sound identification.

Identifications obtained in each experiment are presented respectively in tables 6 and 7. In each table we present the number of the spot, the name of the identified protein, its accession number and database from which it was identified, as well as the theoretical molecular masses and isoelectric point, the number of peptides matched by MS and MS/MS, the sequence coverage and the identification score.

Table 6: B5H/Wt assay identification table

Spot reference	Protein name	Species	Software/Data base[1]	Accession number	Protein MM (Da)	PI	Matched peptides[2]		Sequence coverage (%)[3]	Score[4]
							MS	MS/MS		
8671	Carbonic anhydrase	*Nicotiana tabacum*	GPS/Uniref	P27141	34888	6.41	3	1	14	156
8949	Actin-53	*Nicotiana tabacum*	GPS/SwissProt Green Plants	ACT2_TOBAC	37460.1	5.39	4	2	14	132
8919	Phosphoglycerate kinase	*Nicotiana tabacum*	GPS/Uniref	Q42961	50316.9	8.48	7	4	16	287
9105	Fructose-bisphosphate aldolase	*Nicotiana paniculata*	GPS/Uniref	Q9SXX4	42832	6.92	3	2	7	153
9235	Phosphoglycerate kinase	*Nicotiana tabacum*	GPS/SwissProt Green Plants	PGKH_TOBAC	50316.9	8.48	5	2	10	119
9156	Glyceraldehyde-3-phosphate dehydrogenase A	*Nicotiana tabacum*	GPS/Uniref	P09043	42121.78	6.6	2	1	4	131
9237	Glyceraldehyde-3-phosphate dehydrogenase A	*Nicotiana tabacum*	GPS/Uniref	P09043	42121.8	6.6	5	3	14	351
9146	alkyl hydroperoxide reductase	*Burkholderia sp.*	Protein pilot/NCBI	gi|78066720	20486	5.15	7	-	18	260

9107	glyceraldehyde-3-phosphate dehydrogenase	*Vicia sativa*	GPS/NCBI	gi|296784038	40425.1	8.56	4	2	9	101
9171	GDP-mannose 3',5'-epimerase	*Solanum lycopersicum*	GPS/uniref	C6K2K9	42827.9	5.88	4	3	14	270
8512	Ribulose-1,5-Bisphosphate Carboxylase/oxygenase	Nicotiana tabacum	Protein pilot/NCBI	gi|30013663	20496	7.57	5	-	12	131
8611	Ribulose-1,5-Bisphosphate Carboxylase/oxygenase	*Nicotiana Tabacum*	GPS/NCBI	gi|230922	14550.2	5.19	3	1	18	102
8675	Ribulose bisphosphate carboxylase small chain	*Nicotiana Tabacum*	GPS/NCBI	gi|231070	14478.2	5.42	3	2	13	212
3697	phosphoglycerate kinase	Nicotiana benthamina	Protein pilot/NCBI	gi|313585890	50224;	7.66	4	-	4	121
9125	Glyceraldehyde-3-phosphate dehydrogenase A	*Nicotiana tabacum*	GPS/Swissprot	G3PA_TOBAC	42121.8	6.6	5	1	10	118
9247	Glyceraldehyde-3-phosphate dehydrogenase A	*Nicotiana tabacum*	GPS/swissprot	G3PA_TOBAC	42121.8	6.6	6	2	14	123
8704	Glyceraldehyde-3-phosphate dehydrogenase A	*Nicotiana tabacum*	GPS/NCBI	gi|4539543	36702.1	7.7	8	4	20	133
8476	Fructose-bisphosphate aldolase	*Nicotiana paniculata*	GPS/Uniref	Q9SXX4	42832	6.92	7	3	17	324
9174	chloroplast oxygen-evolving protein 16 kDa subunit	*Nicotiana tabacum*	GPS/NCBI	gi|58700509	24178.9	9.72	1	1	9	96

[1]: software and database from where the identification was made, [2]: Number of peptides, matching the identified protein, whose sequence differs in at least one amino acid residue.by both MS and MS/MS; [3] Percentage of the identified protein sequence covered by the matched peptides; [4]: Protein score, obtained by Mowse algorithm is -10*Log(P), where P is the probability that the observed match is a random event. Protein scores considered significant (p<0.05) depend on the database (score of at least 85 (NCBInr and UniRef100); 70 (SwissProt); 67 (Medicago) and 58 (SwissProt 2012 restricted to Viridiplantae (Green Plants)). Mascot search engine calculated the significance ($\mathbf{p} < 0{,}05$) for the database used).

Table 7: B1F/Wt assay identification table

Spot reference	Protein name	species	Software/ Data base[1]	Accession number	Protein MM (Da)	PI	Matched peptides[2]		Sequence coverage (%)	Score[3]
							MS	MS/MS		

2220	ribulose-1,5-biphosphate carboxylase/ oxygenase large subunit	*Nicotiana tabacum*	GPS/NCBI	gi|11465965	52864.8	6.41	14	6	36	991
2201	ribulose-1,5-biphosphate carboxylase/ oxygenase large subunit	*Nicotiana tabacum*	Protein pilot (NCBI)	gi|11465965	53378	6.41	28	-	33	914
5470	ribulose-1,5-biphosphate carboxylase/ oxygenase large subunit	*Nicotiana tabacum*	GPS/NCBI	gi|11465965	52864.8	6.41	13	7	30	776
5834	Ribulose bisphosphate carboxylase/oxygenase activase 2	*Nicotiana tabacum*	GPS/Uniref	Q40565	48540.6	8.14	8	5	23	729
5756	Ribulose bisphosphate carboxylase/oxygenase activase 1	*Nicotiana tabacum*	GPS/Uniref	Q40460	48950.9	8.44	4	1	4	87
5798	Ribulose bisphosphate carboxylase/oxygenase activase 2	*Nicotiana tabacum*	GPS/Uniref	Q40565	48540.6	8.14	9	6	23	748
5574	Phosphoglycerate kinase	*Nicotiana tabacum*	GPS/Uniref	Q42961	50316.9	8.48	6	2	15	330
5744	Phosphoglycerate kinase	*Nicotiana tabacum*	GPS/Uniref	Q42961	50316.9	8.48	7	5	18	580
5831	Fructose-bisphosphate aldolase	*Nicotiana tabacum*	GPS/Uniref	F2VJ75	43064	6.38	3	1	9	121
5624	Glyceraldehyde-3-phosphate dehydrogenase A	*Nicotiana tabacum*	GPS/Uniref	P09043	42121.8	6,6	4	2	10	213
5838	Glyceraldehyde-3-phosphate dehydrogenase A	*Nicotiana tabacum*	GPS/Uniref	P09043	42121.8	6,6	5	3	14	411
5674	GDP-mannose 3',5'-epimerase	*Solanum lycopersicum*	Protein pilot/NCBI	gi|350539619	42828	5.88	7	-	11	287
5666	Glyceraldehyde-3-phosphate dehydrogenase B	*Nicotiana tabacum*	GPS/Uniref	P09044	47953.6	8.83	2	1	6	98
5769	glyceraldehyde 3-phosphate dehydrogenase	*Euphorbia calcarata*	Protein pilot/NCBI	gi|167781847	4969	9.41	3	-	44	177

5736	Glyceraldehyde-3-phosphate dehydrogenase	*Nicotiana tabacum*	GPS/Uniref	Q9XG67	36816.1	7.7	4	1	10	251
5731	Aminomethyltransferase	*Solanum tuberosum*	GPS/Uniref	P54260	44647.8	8.77	6	1	16	138
5476	Aminomethyltransferase	*Solanum tuberosum*	GPS/Uniref	P54260	44647.8	8.77	3	1	6	109
5839	oxygen evolving complex 33 kDa photosystem II protein	*Nicotiana tabacum*	GPS/NCBI	gi|30013657	35145.9	5.61	5	2	18	282
5699	oxygen evolving complex 33 kDa photosystem II protein	*Nicotiana tabacum*	GPS/NCBI	gi|30013657	35176.9	5.63	6	3	25	401
5358	Ribulose bisphosphate carboxylase small chain	*Nicotiana tabacum*	GPS/Uniref	Q84QE5	20496.2	7.57	4	1	20	142
5625	Phosphoglycerate kinase	*Nicotiana tabacum*	GPS/SwissProt Green plants	PGKH_TOBAC	50317	8.48	2	1	3	78
5379	Ribulose bisphosphate carboxylase small chain	*Medicago sativa*	GPS/SwissProt Green Plants	RBS_MEDSA	20466	8.86	2	1	12	61
5837	Ribulose bisphosphate carboxylase small chain	*Nicotiana tabacum*	GPS/Swissprot	RBS_TOBAC	20526.2	7.6	6	3	27	270
5803	Fructose-bisphosphate aldolase	*Nicotiana paniculata*	GPS/Uniref	Q9SXX4	42832	6.92	4	2	9	178
5542	beta-carbonic anhydrase	*Nicotiana tabacum*	GPS/Uniref	P27141	34887.8	6.41	4	-	12	94
5495	hydroxypyruvate reductase	*Arabidopsis thaliana*	GPS/NCBI	gi|15220620	42221	6.68	5	3	11	85

[1]: software and database from where the identification was made,
[2]: Number of peptides, matching the identified protein, whose sequence differs in at least one amino acid residue by both MS and MS/MS;
[3] Percentage of the identified protein sequence covered by the matched peptides;
[4]: Protein score, obtained by Mowse algorithm is -10*Log(P), where P is the probability that the observed match is a random event. Protein scores considered significant (p<0.05) depend on the data base (score of at least 85 (NCBInr and UniRef100); 70 (SwissProt); 67 (Medicago) and 58 (SwissProt 2012 restricted to Viridiplantae (Green Plants)). Mascot search engine calculated the significance ($p < 0,05$) for the database used).

4 Discussion

As we aimed to study the effects of a Cd exposure in the transgenic tobacco lines B5H and B1F when comparing to the wild types, we used a 2-DE-DIGE based strategy followed by identification of differentially expressed proteins using mass spectrometry. The variation patterns, of the identified proteins, detected in the image analysis will be subsequently discussed by function in plants and the variation in the each line will be compared with those of the Wild type.

Carbonic anhydrase (CA)

CA is a zinc-containing metalloenzyme that in numerous organisms catalyzes the interconversion of $C0_2$ and $HC0_3^-$. It is required in biological systems to increase the flux rates between these biochemical species, essential for carbon fixation. In higher plants, CA is required for photosynthesis and additionally almost all the $C0_2$ that is fixed must pass through the CA-catalyzed reaction[56].

In this work CA was showed differential expression in both assays [spot number 8671 (B5H/Wt assay) and Spot number 5542 (B1F/Wt assay)]. In the B5H/Wt assay, the expression of Carbonic anhydrase enzyme, in the Wt Cd exposed had an increase of over 7 fold relatively to the control, whereas in B5H plants there was no significant difference of expression as shown in figure A1. For the B1F/Wt assay Wt Cd exposed plants also had an increase of over 5 fold, by comparison to controls whereas in the B1F plants, the expression in the control was significantly higher than the Wt in the same condition but when subjected to cadmium exposure shows a decrease to levels close to Wt control plants, as shown in figure A2.

By its affinity for thiol and ability to replace particular trace elements, that play the part of coenzymes, cadmium has been described to directly or indirectly, the activity of carbonic anhydrase[57]. In fact, it may be hypothesized that by substituting Zinc as a cofactor in carbonic anhydrase, cadmium may inhibit the activity of this enzyme. Consequently, in an effort to keep CA determinant role, and under heavy-metal stress, the plants would tend to over-express this enzyme. As the expression of B5H plants does not suffer any alteration, the results presented to CA suggests that the carbon fixation is not much affected by the presence of the metal in these plants, indicating

that B5H plants could have more tolerance to cadmium contamination than Wt plants and also denotes that B1F plants may have an ability to endure more efficiently, in terms of carbon fixation, the contamination by cadmium.

Ribulose 1,5-bisphosphate carboxylase/oxygenase (RuBisCO)

The carbon fixation reaction results in the formation of two molecules 3-phosphoglycerate (PGA) that are integrated into the Calvin cycle ultimately to form sugars. During oxygen fixation, one molecule of PGA and one molecule of 2-phosphoglycolate are formed. The latter is converted back to PGA in the photorespiratory cycle. The Ribulose 1, 5-bisphosphate carboxylase/oxygenase (RuBisCO) initiates the photosynthetic carbon metabolism by determining the rate at which CO2 is incorporated into sugar phosphate through the carboxylation of RuBP (Ribulose Biphosohate). The entrance reactions to both photosynthesis and photorespiration are catalyzed by RuBisCO. It exists in higher plants as a large macromolecular complex of eight large and eight small subunits. [58,59]

In the B5H/Wt assay we found three spots identified as RuBisCO small subunit (8512, 8611 and 8675), whereas in B1F/Wt assay three spots as RuBisCO large subunit (2220, 2201 and 5470) and other three identified as small subunit (5368, 5379 and 5837). In the B5H/Wt assay, the expression of RuBisCO small subunit had an increase in the Wt plants submitted to cadmium (average 2.27 fold) in relation to the control whereas in the B5H plants there in no significant variation as shown in figure A3. In the B1F/Wt assay, the spots identified as RuBisCO large subunit, although they all shown an increase in the Wt submitted to cadmium stress in relation to Wt controls and a decrease in the B1F plants, they present different patterns of variation as shown in figure A4. This observation shows a response, by the B1F plants to the stress contrary to the tendency of the Wt plants to increase the expression of the RuBisCO large subunit when in stress; the B1F plants have a higher expression pattern in the control reducing it to levels near Wt control, when subjected to cadmium exposure. As for the spots identified as RuBisCO small unit, we noticed an increase in the Wt plants

submitted to cadmium (average 2.7 fold) in relation with the control whereas in the B5H plants there is a slight decrease in the expression as shown in figure A4 D, E and F.

The results of the Wt plants corroborate those previously described by Farinati and collages that detected eight protein spots showing a statistically significant up-regulation, all belonging to the RuBisCO large subunit, whose induction is particularly marked by the treatment with heavy metals. Similarly to the large subunit, RuBisCO small subunit also was shown to be upregulared in the Farinati experiment. These authors proposed that, heavy metals accumulation in plants has high energy costs to the plant metabolism, and that in order for plants to be able to cope, they respond by reinforcing the photosynthetic mechanism, particularly through the over-expression of proteins involved in photosynthesis[49]

Consequently, it could be proposed that our results suggest that both transgenic lines are able to tolerate cadmium contamination by comparison to Wt plants as there are no significant increase in the expression patterns of this protein as a consequence of Cadmium exposure. Results seem also to point out that such tolerance is not a direct consequence of trehalose-6-phosphate synthase expression and consequently putative trehalose accumulation as both transgenic lines show similar responses.

RuBisCO activase

RuBisCO activase is an ATPase that ultimately determines the proportion of RuBisCO active sites promoting the activation' of RuBisCO by easing the dissociation of sugar phosphates from either decarbamylated sites containing RuBP or analogs of RuBP [60]. Its activity in plants plays a vital role in the reaction of photosynthesis to temperature. As one chaperone functions to promote and maintain the catalytic activity of RuBisCO[61]

The RuBisCO activase was only identified in B1F/Wt assay in three spots [one of RuBisCO activase 1 (5756) and two as RuBisCO activase 2 (5834 and 5798)]; both RuBisCO activase 1 and 2 showed overexpression in Wt plants exposed to cadmium in relation to the control of 2.33 fold. In the B1F plants while the expression of RuBisCO

activase 2 remains unaltered, the expression of RuBisCO activase 1 suffers a significant decrease (0.7 fold the control value) as shown in figure A5. This result is in accordance with those of Hajduch and coworkers and suggest a damaging effect on the photosynthetic apparatus as a consequence of Cadmium accumulation[46] that as a consequence leads to an over-expression in wild type plants of RuBisCO activase and as seen previously in both RuBisCO large and small units in a plant's effort to counter such damages. Interestingly, such expression increase is not recorded in B1F transgenic plants that seem to maintain the initial expression levels of this enzyme, probably maintaining their photosynthetic efficiency.

Oxygen evolving complex (OEC)

The oxygen evolving complex-33 KDa (OEC) occurs in the thylakoid membrane together with many other protein subunits, with roles in light harvesting, photoprotection, structural stability, among others. As the oxidizing side of Photosystem II, catalyses the oxidation of water to O2 in a multistep process that requires Ca2+ and Cl- for proper function of the catalytic centre. In higher plants two additional subunits the OEC-23 KDa and the OEC-16 KDa are described [47].

In spot 9174, of the B5H/Wt assay, a 16-KDa subunit of the OEC was identified as shown in figure A6. In spite of the expression of this protein B5H control was higher than the one for the Wt under the same condition; there is no expression variation in the B5H plant while in Wt plants an over expression is noted upon cadmium exposure with a 2.1 fold expression increase. In the B1F/Wt assay two spots of the 33 KDa subunit (spots 5839 and 5699) were identified. The B1F controls present a relatively lower expression of these proteins, when compared with the Wt plants in the same conditions; but when subjected to stress, while in Wt the expression of these proteins drop 1.8 fold the original expression, the B1F plants respond by increasing the expression(1.22 fold average) (Figure A7).

According to Kieffer and co-workers [48], to avoid photo-oxidative damage, the down-regulation of carbon fixation must be counterbalanced by a suppression of photosynthetic electron transport. Concurrently, different proteins of the photosystem

II complex such as the oxygen-evolving enhancer proteins as well as other key proteins are suppressed, as shown by Kieffer et al., (2008). The 33kDa subunit of the OECs results of the Wt plants are according to their findings. The results for this protein suggest that the function of the Photosystem II may not be affected denoting a resistance to heavy metal exposure by the B5H plants. As for the B1F plants the results shown that they respond by increasing the expression, suggesting that these plants can maintain, or even increase the activity of the photosystem II.

hydroxypyruvate reductase

Hydroxypyruvate reductase (HPR) is a leaf peroxisomal enzyme that functions in the glycolate pathway of photorespiration in plants. Photosynthesis depends on the activity of HPR through the recycling of Carbon in the photorespiratory cycle[62,63].

The hidroxipyruvate redutase was identified in the B1F/Wt assay in spot 5495, which shown an increase of 3.5 fold in the Wt plants exposed to cadmium in relation with the control whilst the B1F plants shown a decrease in the expression. As shown in figure A8. Farinati and co-workers also found a higher HPR expression in cadmium treated plants, stating that this is likely due to the higher RuBisCO content[49]. The same reason could be stated here, indicating that transgenic plants engineered with the AtTPS1 gene seem to be able to withstand better Cadmium toxicity.

Glyceraldehyde-3-phosphate dehydrogenase (GAPDH)

In B5H/Wt assay GAPDH was identified in four spots (9237; 9125; 9247 and 8704) and in five spots in the B1F/Wt (8624; 5838; 5666; 5769 and 5736) experiment. For the B5H assay in the Wt plants there is a significant increase in the expression of this protein (in average 2.8 fold) whereas in the B5H plants the increase is not significant as shown in figure A9. In the B1F/Wt assay, in the Wt plants the increase is approximately the same as in B5H/Wt assay (in average 2.88 fold) while in the B1F plants in noticed a significant decrease in most of the spots identified as GAPDH as shown in figure A10

Glyceraldehyde-3-phosphate dehydrogenases catalyze key steps in energy and reducing power partitioning in cells of higher plants. The glycolytic glyceraldehyde-3-

phosphate dehydrogenase (GAPDH) is a multifaceted protein that is involved in numerous processes including glycolysis, translational silencing, transcriptional regulation of specific genes, and acting as a nitric oxide sensor as well as apoptosis. It reversibly converts glyceraldehyde-3- phosphate to 1,3-bisphosphoglycerate by coupling with the reduction of NAD^+ to NADH[64–66].

Wt results are according to the communication made by Vescovi and team in which they demonstrated that GAPDH activity increased in response to cadmium induced oxidative stress, and thus it could be used as a stress sensor[67].The result regarding the spots recognized as Glyceraldehyde-3-phosphate dehydrogenase revealed that both B5H and B1F strains had the same behavior in the expression pattern of this protein, leading to consider that both have the ability to endure cadmium stress better than Wt plants.

Phosphoglycerate kinase PGK

Phosphoglycerate kinase (PGK) is an enzyme implicated in the glicolytic pathway and Calvin cycle with formation of ATP from ADP[68,69], catalyzing the reversible conversion of 1,3- bisphosphoglycerate to 3-phosphoglycerate (3PG) during.

Three spots were identified as PGK in the B5H/Wt assay (8919; 9235 and 3697) and another 3 spots in B1F/Wt assay (5574; 5744 and 5625). In the B5H/Wt assay the expression of PGK enzyme, in the Wt Cd exposed have a significant increase (average 3.1 fold) relatively to the control whereas in the B5H plants tended to maintain the levels of expression as seen in figure A11. In the B1F/Wt assay, a similar situation was recorded for both Wt and transgenic lines, a significant increase (2.63 fold) in Wt when exposed to Cd stress and the maintenance of the expression levels in B1F. Such results for PGK are in accordance with the previously mentioned results for RuBisCO and RuBisCO activase, pointing out to the maintenance of photosynthetic capacity in transgenic plants when subjected to Cadmium stress.

Fructose-bisphosphate aldolase (FBPA)

There were 2 spots identified as Fructose-bisphosphate aldolase in the B5H/Wt assay (9105 and 8476) and another two in B1F/Wt assay (5831 and 5803). In the B5H/Wt

assay, Wt plants shown a significant increase in the expression of FBPA in the cadmium treated plants, when compared to the control (average 2.75 fold), whilst in the B5H plants subjected to Cd stress, a slight decrease was detected, as shown in figure A12.

FBPA is a glycolitic enzyme that catalyses the interconversion of fructose 1, 6-bisphosphate into glyceraldehyde 3-phosphate and dihydroxyacetone phosphate. FBPA enzymes have been found in a broad range of eukaryotic and prokaryotic organisms[70]. In the B1F/Wt assay, Wt plants shown a significant increase in the expression of FBPA in the cadmium treated plants, when compared to the control (average 2.15 fold), while in the B1F plants it was noticed a slight decrease as shown in figure A7.

As referred above GAPD, one of the glycolitic enzymes, have known activities in the apoptotic signaling as Kim reported GAPD expression was significantly increased during apoptosis, which was induced by various factors including prolonged culture, nutrient removal and cytotoxic agents[66]. Like GAPD other glycolitic enzymes could have similar roles. We can infer, that in Wt plants the overexpression patterns of the glycolitic enzymes could be reveling of an apoptotic activity, also the enhanced tolerance of the B1F and B5H plants.

GDP-mannose 3',5'-epimerase (GME)

GDP-mannose-3',5'-epimerase catalyses the epimerization (the change of one epimeric form of a compound into another, as by enzymatic action, being a epimer an stereoisomer which differ in the orientation of a single asymmetric carbon) of both the 3' and 5' positions of GDP-α-D-mannose to yield GDP-β-L galactose. It was confirmed that GME establishes equilibrium between two products, GDP- β -L-galactose and GDP- β -L-glucose [71,72].

One spot was identified as GDP-mannose 3',5'-epimerase (GME) in the B5H/Wt assay (9171) and in the B1F/Wt assay (5674). In the B5H/Wt assay in the Wt plants there is a significant increase in the expression of this protein (1.8 fold) while in the B5H plants there is no variation, as shown in figure A12 A. In the B1F/Wt assay in the Wt plants there is a significant increase in the expression of this protein (2 fold) while in the B1F, similarly to B5H plants, there is no significant variation as shown in figure A13 B. The

results from Zhang and team suggested that the overexpression GME result in increased ascorbate accumulation in tomato which improved tolerance to abiotic stresse[73]. In our results GME expression was higher in Wt treated with cadmium denoting a stress response. As in both B1F and B5H plants there is no variation in the expression of this protein. These results lead us to conclude that they are tolerant to this level of cadmium exposure.

Aminomethyltransferase

Aminomethyltransferase, a component of the glycine cleavage system it degrades the aminomethyl moiety of glycine to ammonia and 5, 10-methylenetetrahydrofolate in the presence of tetrahydrofolate. [74].

Aminomethiltransferase was identified only in B1F/Wt assay (spot 5731) and for this spot, as in other identified proteins the expression of it in Wt plants exposed to cadmium in relation to the control significantly increased (2,9 fold), whereas in B1F plants the expression slightly decreased, as shown in figure A14. As for B1F plants, despite of having an expression slightly higher than the Wt in the same condition; when submitted to cadmium contamination the expression fall to a level similar to those of controls. Falvo and co-workers demonstrated that Aminomethiltransferase, plays a major role in plant metabolism being essential for biosynthesis of methionine, pyrimidines and purines and stress responses [75] and that, in addition, plants subjected to Cd stress increase the expression levels. The results obtained in this experiment seem to be in accordance with this results and seem to point to an increased expression in Wt plants whereas transgenic line B1F is able to cope with abiotic stress more effectively maintain the expression of this enzyme.

Alkyl-hydroperoxide-reductase

Alkyl-hydroperoxide-reductases are proteins from the Peroxiredoxin family and had received considerable attention in recent years as a new and expanding family of thiol-specific antioxidant, exerting their protective antioxidant role in cells through their

peroxidase activity, where hydrogen peroxide, peroxynitrite and a wide range of organic hydroperoxides are reduced and detoxified. Although these proteins are primarily located in the cytosol, they are also found within mitochondria, chloroplasts and peroxisomes, associated with nuclei and membranes[76]. As an enzyme with an antioxidant role, it is expected to be over expressed when the plants are subjected to stress. This is in accordance to the results obtained in our experiment where an increase in both Wt and B5H plants submitted to cadmium relatively to the controls. Nevertheless, it is noteworthy that in B5H plants such increase is much smaller (figure A15). This suggests that the response to oxidative stress is less pronounced in the transgenic B5H line.

5 General Conclusions and Future Prospects

In all the spots identified as proteins involved in photosynthesis, the same patterns of variation were found, suggesting that the photosynthesis and carbon fixation in both B1F and B5H plants is more effective under Cadmium induced stress than in Wt plants. Nevertheless B1F plants show signals of having more tolerance to stress than B5H in terms of photosynthetic efficiency, as seen in particular for proteins Carbonic anhydrase and RuBisCO.small unit

The same consistent variation patterns were found in the identified glycolitic proteins. Suggesting, as stated earlier that in Wt plants the overexpression patterns of the glycolitic enzymes could be reveling of an apoptotic activity, also the enhanced tolerance of the B1F and B5H plants.

In this work we could identify a total of fifteen different proteins and all the results demonstrate that both transgenic lines present an enhanced tolerance to cadmium induced stress, showing signals which denote that they may not be as affected as Wt plants. It may therefore be considered that genetic engineering with the trehalose-6-phosphate synthase increases tolerance to Cadmium induced stress in transgenic plants, similarly to what was described for water deficit stress. In addition, it could be suggested that such an approach may be of use in the transformation of fiber

production plants that could be grown in Cd contaminated soils as well as for phytoremediation.

Furthermore, it would be interesting to see the expression variation patterns of plants exposed to higher concentrations of cadmium, to confirm if the tendency revealed in the results is maintained and if so, up to which level. Such results could be related to other physiological data, namely photosynthesis levels. As Cd uptake is done at the level of the roots, it would also be interesting to conduct such an approach at the root level. It would also be interesting to test other metals such as those tested by Batista in 2009 in order to understand if proteomic results are comparable.

Finally, for a full assessing on how these plants are effectively able to cope with Cd-induced stress, it would be important to conduct this approach in soil conditions.

6 Bibliography

1. Ipeaiyeda AR, Dawodu M. Heavy Metals Contamination Of Topsoil And Dispersion In The Vicinities Of Reclaimed Auto-Repair Workshops In Iwo, Nigeria. *Chemical Society of Ethiopia*. 2008;22(3):339–348.

2. Sa'ad NS, Artanti R, Dewi T. Phyto-Remediation For Rehabilitation Of Agricultural Land Contaminated By Cadmium And Copper. *Phyto-remediation for rehabilitatio*. 2011;4(1):17–21.

3. Montinaro S, Concas A, Pisu M, Cao G. Remediation of heavy metals contaminated soils by ball milling. *Chemosphere*. 2007;67(4):631–9. Available at: http://www.ncbi.nlm.nih.gov/pubmed/17188323.

4. Singh R, Singh D, Kumar N. Accumulation and translocation of heavy metals in soil and plants from fly ash contaminated area. *Journal of Environmental Biology*. 2010;430(July):421–430. Available at: http://jeb.co.in/journal_issues/201007_jul10/paper_07.pdf. Accessed October 14, 2012.

5. Körpe DA, Aras S. Evaluation of copper-induced stress on eggplant (Solanum melongena L.) seedlings at the molecular and population levels by use of various biomarkers. *Mutation research*. 2011;719(1-2):29–34. Available at: http://www.ncbi.nlm.nih.gov/pubmed/20970520. Accessed August 28, 2012.

6. Memon AR, Schröder P. Implications of metal accumulation mechanisms to phytoremediation. *Environmental science and pollution research international*. 2009;16(2):162–75. Available at: http://www.ncbi.nlm.nih.gov/pubmed/19067014. Accessed July 26, 2012.

7. Yang Z, Chu C. Towards Understanding Plant Response to Heavy Metal Stress. In: *Abiotic Stress in Plants – Mechanisms and Adaptations*.; 2008:59–78. Available at: http://www.intechopen.com/source/pdfs/18398/InTech-Towards_understanding_plant_response_to_heavy_metal_stress.pdf. Accessed September 7, 2012.

8. Bona E, Marsano F, Massa N, Cattaneo C, Cesaro P, Argese E, Di Toppi L, Cavaletto M, Berta G. Proteomic analysis as a tool for investigating arsenic stress in Pteris vittata roots colonized or not by arbuscular mycorrhizal symbiosis. *Journal of proteomics*. 2011;74(8):1338–1350. Available at: http://www.ncbi.nlm.nih.gov/pubmed/21457805.

9. Nwugo C, Huerta A. The effect of silicon on the leaf proteome of rice (Oryza sativa L.) plants under cadmium-stress. *Journal of Proteome Research*. 2011:518–528. Available at: http://pubs.acs.org/doi/abs/10.1021/pr100716h. Accessed August 28, 2012.

10. Aloui A, Recorbet G, Robert F, Schoefs B, Bertrand M, Henry C, Gianinazzi-Pearson V, Dumas-Gaudot E, Aschi-Smiti S. Arbuscular mycorrhizal symbiosis elicits shoot proteome changes that are modified during cadmium stress alleviation in Medicago truncatula. *BMC plant biology*. 2011;11(1):75. Available at: http://www.pubmedcentral.nih.gov/articlerender.fcgi?artid=3112074&tool=pmcentrez&rendertype=abstract. Accessed August 28, 2012.

11. Lee K, Bae DW, Kim SH, Han H, Liu X, Park H, Lim C, Lee S, Chung W. Comparative proteomic analysis of the short-term responses of rice roots and leaves to cadmium. *Journal of plant physiology*. 2010;167(3):161–8. Available at: http://www.ncbi.nlm.nih.gov/pubmed/19853963. Accessed July 23, 2012.

12. Singh LP, Gill SS, Tuteja N. Unraveling the role of fungal symbionts in plant abiotic stress tolerance. *Plant signaling & behavior*. 2011;6(2):175–91. Available at: http://www.pubmedcentral.nih.gov/articlerender.fcgi?artid=3121976&tool=pmcentrez&rendertype=abstract.

13. Gill SS, Tuteja N. Cadmium stress tolerance in crop plants: probing the role of sulfur. *Plant signaling behavior*. 2011;6(2):215–222. Available at: http://www.landesbioscience.com/journals/psb/article/14880/.

14. Sarry J-E, Kuhn L, Ducruix C, Lafaye A, Junot C, Hugouvieux V, Jourdain A, Bastien O, Fievet J, Vailhen D, Amekraz B, Moulin C, Ezan E, Garin J, Bourguignon J. The early responses of Arabidopsis thaliana cells to cadmium exposure explored by protein and metabolite profiling analyses. *Proteomics*. 2006;6(7):2180–98. Available at: http://www.ncbi.nlm.nih.gov/pubmed/16502469. Accessed October 16, 2012.

15. Venkateswarlu B. Abiotic Stress In Plants – Mechanisms And Adaptations. In: *Abiotic Stress in Plants – Mechanisms and Adaptations*. InTech; 2011.

16. Almeida AM, Cardoso L a., Santos DM, Torné JM, Fevereiro PS. Trehalose and its applications in plant biotechnology. *In Vitro Cellular & Developmental Biology - Plant*. 2007;43(3):167–177. Available at: http://www.springerlink.com/index/10.1007/s11627-006-9024-3. Accessed August 2, 2012.

17. Paul MJ, Primavesi LF, Jhurreea D, Zhang Y. Trehalose metabolism and signaling. *Annual review of plant biology*. 2008;59:417–41. Available at: http://www.ncbi.nlm.nih.gov/pubmed/18257709. Accessed August 10, 2012.

18. Ohtake S, Wang Y. Trehalose: current use and future applications. *Journal of pharmaceutical sciences*. 2011;100(6):2020–2053. Available at: http://onlinelibrary.wiley.com/doi/10.1002/jps.22458/full. Accessed August 28, 2012.

19. Iordachescu M, Imai R. *Trehalose and Abiotic Stress in Biological Systems*. 2008. Available at: http://www.intechopen.com/source/pdfs/18404/InTech-Trehalose_and_abiotic_stress_in_biological_systems.pdf. Accessed August 28, 2012.

20. Avonce N, Mendoza-Vargas A, Morett E, Iturriaga G. Insights on the evolution of trehalose biosynthesis. *BMC evolutionary biology*. 2006;6:109. Available at: http://www.pubmedcentral.nih.gov/articlerender.fcgi?artid=1769515&tool=pmcentrez&rendertype=abstract. Accessed July 17, 2012.

21. Almeida AM, Silva AB, Araújo SS, Cardoso L, Santos D, Torné J, Silva J, Paul M, Fevereiro P. Responses to water withdrawal of tobacco plants genetically engineered with the AtTPS1 gene: a special reference to photosynthetic parameters. *Euphytica*. 2006;154(1-2):113–126. Available at: http://www.springerlink.com/index/10.1007/s10681-006-9277-2. Accessed August 28, 2012.

22. Almeida AM, Villalobos E, Araújo SS, Leyman B, Dijck P, Alfaro-Cardoso L, Fevereiro P, Torné J, Santos D. Transformation of tobacco with an Arabidopsis thaliana gene involved in trehalose biosynthesis increases tolerance to several abiotic stresses. *Euphytica*. 2005;146(1-2):165–176. Available at: http://www.springerlink.com/index/10.1007/s10681-005-7080-0. Accessed August 28, 2012.

23. Grennan AK. The role of trehalose biosynthesis in plants. *Plant physiology*. 2007;144(1):3–5. Available at: http://www.pubmedcentral.nih.gov/articlerender.fcgi?artid=1913774&tool=pmcentrez&rendertype=abstract. Accessed July 13, 2012.

24. Ganapathi TR, Suprasanna P, Rao PS, Bapat VA. Tobacco (Nicotiana tabacum L .) -A model system for tissue culture interventions and genetic engineering. *Indian Journal of Biotechnology*. 2004;3(April):171–184.

25. FloriDazL™. Floridata: Nicotiana tabacum. *Plant Encyclopedia*. 2012. Available at: http://www.floridata.com/ref/n/nico_tab.cfm. Accessed October 17, 2012.

26. Thelen J. Introduction to proteomics: A brief historical perspective on contemporary approaches. In: *Plant Proteomics, Springer, Berlin*.; 2007:1–6. Available at: http://content.schweitzer-online.de/static/content/catalog/newbooks/978/354/072/9783540726166/9783540726166_Excerpt_001.pdf. Accessed October 17, 2012.

27. Schulze WX, Usadel B. Quantitation in mass-spectrometry-based proteomics. *Annual review of plant biology*. 2010;61:491–516. Available at: http://www.ncbi.nlm.nih.gov/pubmed/20192741. Accessed July 14, 2012.

28. Timms JF, Cramer R. Difference gel electrophoresis. *Proteomics*. 2008;8(23-24):4886–97. Available at: http://www.ncbi.nlm.nih.gov/pubmed/19003860. Accessed July 31, 2012.

29. Lilley KS, Dupree P. Methods of quantitative proteomics and their application to plant organelle characterization. *Journal of experimental botany*. 2006;57(7):1493–9. Available at: http://www.ncbi.nlm.nih.gov/pubmed/16617121. Accessed August 27, 2012.

30. Healthcare GE. *2-D Electrophoresis*. 2004.

31. Oeljeklaus S, Meyer HE, Warscheid B. Advancements in plant proteomics using quantitative mass spectrometry. *Journal of proteomics*. 2009;72(3):545–554. Available at: http://www.ncbi.nlm.nih.gov/pubmed/19049910.

32. Bindschedler LV, Cramer R. Quantitative plant proteomics. *Proteomics*. 2011;11(4):756–775. Available at: http://dx.doi.org/10.1002/pmic.201000426.

33. Healthcare G. User Manual.

34. Liebler DC. *Introduction to Proteomics, Tools for the New Biology*. 2012. Available at: http://www.ncbi.nlm.nih.gov/pubmed/23070754.

35. Fuchs B, Süss R, Schiller J. An update of MALDI-TOF mass spectrometry in lipid research. *Progress in lipid research*. 2010;49(4):450–75. Available at: http://www.ncbi.nlm.nih.gov/pubmed/20643161. Accessed July 17, 2012.

36. Wang H-Y, Chu X, Zhao Z-X, He X-S, Guo Y-L. Analysis of low molecular weight compounds by MALDI-FTICR-MS. *Journal of chromatography. B, Analytical technologies in the biomedical and life sciences*. 2011;879(17-18):1166–79. Available at: http://www.ncbi.nlm.nih.gov/pubmed/21482202. Accessed August 28, 2012.

37. Lewis J, Wei J, Siuzdak G. Matrix Assisted Laser Desorption/Ionization Mass Spectrometry in Peptide and Protein Analysis. In: *Encyclopedia of analytical Chemistry*.; 2006:5880–5894. Available at: http://onlinelibrary.wiley.com/doi/10.1002/9780470027318.a1621/full. Accessed October 1, 2012.

38. Gobom J, Nordho E, Mirgorodskaya E, Ekmanb R. Sample PuriÐcation and Preparation Technique Based on Nano-scale Reversed-phase Columns for the Sensitive Analysis of Complex Peptide Mixtures by Matrix-assisted Laser Desorption / Ionization Mass Spectrometry. *Journal of Mass Spectrometry*. 1999;116(July 1998):105–116.

39. Goddijn OJ, Verwoerd TC, Voogd E, Krutwagen R W, de Graaf P T, van Dun K, Poels J, Ponstein A, Damm B, Pen J. Inhibition of trehalase activity enhances trehalose accumulation in transgenic plants. *Plant physiology*. 1997;113(1):181–90. Available at: http://www.pubmedcentral.nih.gov/articlerender.fcgi?artid=158129&tool=pmcentrez&rendertype=abstract.

40. Romero C, Bellés JM, Vayá JL, Serrano R, Culiáñez-Macià FA. Expression of the yeast trehalose-6-phosphate synthase gene in transgenic tobacco plants: pleiotropic phenotypes include drought tolerance. *Planta*. 1997;201(3):293–7. Available at: http://www.ncbi.nlm.nih.gov/pubmed/19343407. Accessed October 17, 2012.

41. Yeo ET, Kwon HB, Han SE, Yeo E T, Kwon H B, Han S E, Lee J T, Ryu J C, Byu M O. Genetic engineering of drought resistant potato plants by introduction of the trehalose-6-phosphate synthase (TPS1) gene from Saccharomyces cerevisiae. *Molecules and cells*. 2000;10(3):263–8. Available at: http://www.ncbi.nlm.nih.gov/pubmed/10901163. Accessed October 17, 2012.
42. Garg AK, Kim J-K, Owens TG, Ranwala A, Choi Y, Kochian L, Wu R. Trehalose accumulation in rice plants confers high tolerance levels to different abiotic stresses. *Proceedings of the National Academy of Sciences of the United States of America*. 2002;99(25):15898–903. Available at: http://www.pubmedcentral.nih.gov/articlerender.fcgi?artid=138536&tool=pmcentrez&rendertype=abstract.

43. Jang I, Oh S, Seo J, Choi W. -phosphate synthase and trehalose-6-phosphate phosphatase in transgenic rice plants increases trehalose accumulation and abiotic stress tolerance without stunting. *Plant Physiology*. 2003;131(February):516–524. Available at: http://www.plantphysiol.org/content/131/2/516.short. Accessed October 17, 2012.

44. Avonce N, Leyman B. The Arabidopsis trehalose-6-P synthase AtTPS1 gene is a regulator of glucose, abscisic acid, and stress signaling. *Plant physiology*. 2004;136(November):3649–3659. Available at: http://www.plantphysiol.org/content/136/3/3649.short. Accessed August 28, 2012.

45. Li H-W, Zang B-S, Deng X-W, Wang X-P. Overexpression of the trehalose-6-phosphate synthase gene OsTPS1 enhances abiotic stress tolerance in rice. *Planta*. 2011;234(5):1007–18. Available at: http://www.ncbi.nlm.nih.gov/pubmed/21698458. Accessed August 27, 2012.

46. Hajduch M, Rakwal R, Agrawal GK, Yonekura M, Pretova A. High-resolution two-dimensional electrophoresis separation of proteins from metal-stressed rice (Oryza sativa L.) leaves: Drastic reductions/ fragmentation of ribulose-1,5-bisphosphate carboxylase/oxygenase and induction of stress- related proteins. *Electrophoresis*. 2001;22:2824–2831. Available at: http://onlinelibrary.wiley.com/doi/10.1002/1522-2683(200108)22:13%3C2824::AID-ELPS2824%3E3.0.CO;2-C/abstract. Accessed October 23, 2012.

47. Bona E, Marsano F, Cavaletto M, Berta G. Proteomic characterization of copper stress response in Cannabis sativa roots. *Proteomics*. 2007;7(7):1121–30. Available at: http://www.ncbi.nlm.nih.gov/pubmed/17352425. Accessed October 16, 2012.

48. Kieffer P, Dommes J, Hoffmann L, Hausman J-F, Renaut J. Quantitative changes in protein expression of cadmium-exposed poplar plants. *Proteomics*. 2008;8(12):2514–30. Available at: http://www.ncbi.nlm.nih.gov/pubmed/18563750. Accessed October 17, 2012.

49. Farinati S, DalCorso G, Bona E, Corbella M, Lampis S, Cecconi D, Polati R, Berta G, Vallini G, Furini A. Proteomic analysis of Arabidopsis halleri shoots in response to the heavy metals cadmium and zinc and rhizosphere microorganisms. *Proteomics*. 2009;9(21):4837–50. Available at: http://www.ncbi.nlm.nih.gov/pubmed/19810031. Accessed October 16, 2012.

50. Zhao L, Sun Y-L, Cui S-X, Chen M, Yang H-M, Liu H-M, Chai T-Y, Huang F. Cd-induced changes in leaf proteome of the hyperaccumulator plant Phytolacca americana. *Chemosphere*. 2011;85(1):56–66. Available at: http://www.ncbi.nlm.nih.gov/pubmed/21723586. Accessed October 16, 2012.

51. Baptista S. Avaliação da resposta ao stresse oxidativo induzido por cádmio e cobre em plantas de tabaco transformadas e não transformadas. 2009. Available at: https://www.repository.utl.pt/handle/10400.5/1059. Accessed October 5, 2012.

52. Kim ST, Cho KS, Jang YS, Kang KY. Two-dimensional electrophoretic analysis of rice proteins by polyethylene glycol fractionation for protein arrays. *Electrophoresis*. 2001;22(10):2103–9. Available at: http://www.ncbi.nlm.nih.gov/pubmed/11465512.

53. Neuhoff V, Arold N, Taube D, Ehrhardt W. Improved staining of proteins in polyacrylamide gels including isoelectric focusing gels with clear background at nanogram sensitivity using Coomassie Brilliant Blue G-250 and R-250. *Electrophoresis*. 1988;9(6):255–62. Available at: http://www.ncbi.nlm.nih.gov/pubmed/2466658. Accessed August 3, 2012.

54. Ventosa MAL da L. Differential proteomics : a study in Medicago truncatula somatic embryogenesis Differential proteomics : a study in Medicago truncatula somatic embryogenesis. 2010.

55. Franco CDMF. Proteomics based approach to understand tissue regeneration. 2011.

56. Badger MR, Price GD. The Role of Carbonic Anhydrase in Photosynthesis. *Annual Review of Plant Physiology and Plant Molecular Biology*. 1994;45(1):369–392. Available at: http://www.annualreviews.org/doi/abs/10.1146/annurev.pp.45.060194.002101.

57. Gontzea I, Popescu F. The effect of body protein supply on resistance to cadmium. *British Journal of Industrial Medicine,*. 1978;35:154–160.

58. Portis A. Regulation of ribulose 1, 5-bisphosphate carboxylase/oxygenase activity. *Annual review of plant biology*. 1992;43:415–437. Available at: http://www.annualreviews.org/doi/abs/10.1146/annurev.pp.43.060192.002215. Accessed October 20, 2012.

59. Peterhansel C, Horst I, Niessen M, Blume C, Kebeish R, Kürkcüoglu S, Kreuzaler. Photorespiration. In: *The Arabidopsis Book*.; 2010:1–24.

60. Crafts-Brandner SJ, Salvucci ME. Rubisco activase constrains the photosynthetic potential of leaves at high temperature and CO2. *Proceedings of the National Academy of Sciences of the United States of America*. 2000;97(24):13430–5. Available at: http://www.pubmedcentral.nih.gov/articlerender.fcgi?artid=27241&tool=pmcentrez&rendertype=abstract.

61. Portis AR. Rubisco activase - Rubisco's catalytic chaperone. *Photosynthesis research*. 2003;75(1):11–27. Available at: http://www.ncbi.nlm.nih.gov/pubmed/16245090. Accessed October 24, 2012.

62. Mano S, Hayashi M, Nishimura M. Light regulates alternative splicing of hydroxypyruvate reductase in pumpkin. *The Plant journal : for cell and molecular biology*. 1999;17(3):309–20. Available at: http://www.ncbi.nlm.nih.gov/pubmed/10097389.

63. Wingler A, Schaewen AV, Leegood RC, Lea PJ, Quick WP. Regulation of Leaf Senescence by Cytokinin , Sugars , and Light Effects on NADH-Dependent Hydroxypyruvate Reductase. *Plant physiology*. 1998;116:329–335.

64. Palamalai V, Miyagi M. Mechanism of glyceraldehyde-3-phosphate dehydrogenase inactivation by tyrosine nitration. *Protein science : a publication of the Protein Society*. 2010;19(2):255–62. Available at: http://www.pubmedcentral.nih.gov/articlerender.fcgi?artid=2865723&tool=pmcentrez&rendertype=abstract. Accessed October 23, 2012.

65. Bustos DM, Iglesias AA. Phosphate Dehydrogenase from Heterotrophic Cells of Wheat Interacts with 14-3-3 Proteins 1. *Plant Physiology*. 2003;133(December):2081–2088.

66. Kim J-W, Dang CV. Multifaceted roles of glycolytic enzymes. *Trends in biochemical sciences*. 2005;30(3):142–50. Available at: http://www.ncbi.nlm.nih.gov/pubmed/15752986. Accessed October 24, 2012.

67. Vescovi M, Costa A, Zaffagnini M, Trost P, F LOS. Arabidopsis Thaliana Glyceraldehyde-3-Phosphate Dehydrogenase As An Oxidative Stress Sensor. 2011.

68. Inoue R, Biehl R, Rosenkranz T, Fitter J, Monkenbusch M, Radulescu A, Farago B, Richter D Large domain fluctuations on 50-ns timescale enable catalytic activity in phosphoglycerate kinase. *Biophysical journal*. 2010;99(7):2309–17. Available at: http://www.pubmedcentral.nih.gov/articlerender.fcgi?artid=3042550&tool=pmcentrez&rendertype=abstract. Accessed October 19, 2012.

69. Pappu KM, Kunnumal B, Serpersu EH. A new metal-binding site for yeast phosphoglycerate kinase as determined by the use of a metal-ATP analog. *Biophysical journal*. 1997;72(2 Pt 1):928–35. Available at: http://www.pubmedcentral.nih.gov/articlerender.fcgi?artid=1185615&tool=pmcentrez&rendertype=abstract.

70. Gardberg A, Abendroth J, Bhandari J, Sankaran B, Staker B. Structure of fructose bisphosphate aldolase from Bartonella henselae bound to fructose 1,6-bisphosphate. *Acta crystallographica. Section F, Structural biology and crystallization communications*. 2011;67(Pt 9):1051–4. Available at: http://www.pubmedcentral.nih.gov/articlerender.fcgi?artid=3169401&tool=pmcentrez&rendertype=abstract. Accessed October 20, 2012.

71. Major LL, Wolucka BA, Naismith JH. Structure and function of GDP-mannose-3′ ,5′ -epimerase; an enzyme which performs three chemical reactions at the same active site. *Journal of The American Chemical Society*. 2005;127(51):18309–18320.

72. Muñoz-Bertomeu J, Cascales-Miñana B, Alaiz M, Segura J, Ros R. A critical role of plastidial glycolytic glyceraldehyde-3-phosphate dehydrogenase in the control of plant metabolism and development. *Plant signaling & Behavior*. 2010;5(1):67–69. Available at: http://www.landesbioscience.com/journals/cc/article/10200/. Accessed October 20, 2012.

73. Zhang C, Liu J, Zhang Y, Cai X, Gong P, Zhang J, Wang, T, Li H, Ye Z. Overexpression of SlGMEs leads to ascorbate accumulation with enhanced oxidative stress, cold, and salt tolerance in tomato. *Plant cell reports*. 2011;30(3):389–98. Available at: http://www.ncbi.nlm.nih.gov/pubmed/20981454. Accessed October 24, 2012.

74. Okamura-Ikeda K, Hosaka H, Maita N, Fujiwara K, Yoshizawa A, Nakagawa A, Taniguchi H. Crystal structure of aminomethyltransferase in complex with dihydrolipoyl-H-protein of the glycine cleavage system: implications for recognition of lipoyl protein substrate, disease-

related mutations, and reaction mechanism. *The Journal of biological chemistry*. 2010;285(24):18684–92. Available at: http://www.pubmedcentral.nih.gov/articlerender.fcgi?artid=2881793&tool=pmcentrez&rendertype=abstract. Accessed October 21, 2012.

75. Falvo S, Di Carli M, Desiderio A, Benvenuto, Moglia, America, Lanteri, Acquadro. 2-D DIGE analysis of UV-C radiation-responsive proteins in globe artichoke leaves. *Proteomics*. 2012;12(3):448–60. Available at: http://www.ncbi.nlm.nih.gov/pubmed/22162389. Accessed August 17, 2012.

76. Wood Z a, Schröder E, Robin Harris J, Poole LB. Structure, mechanism and regulation of peroxiredoxins. *Trends in biochemical sciences*. 2003;28(1):32–40. Available at: http://www.ncbi.nlm.nih.gov/pubmed/12517450.

Annex

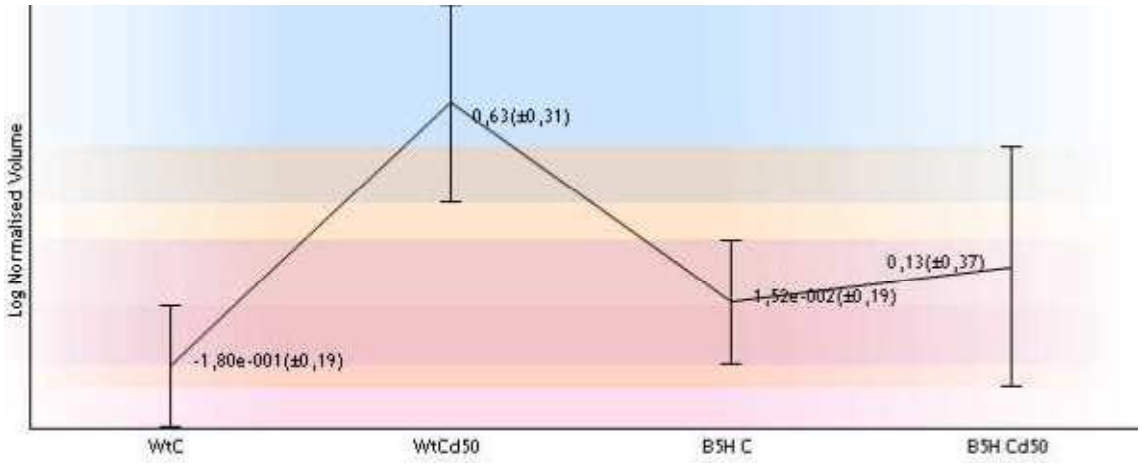

Figure A1: graphic comparing the normalized volumes of the spot 8671 (CA) in each experimental group of the B5H/Wt assay

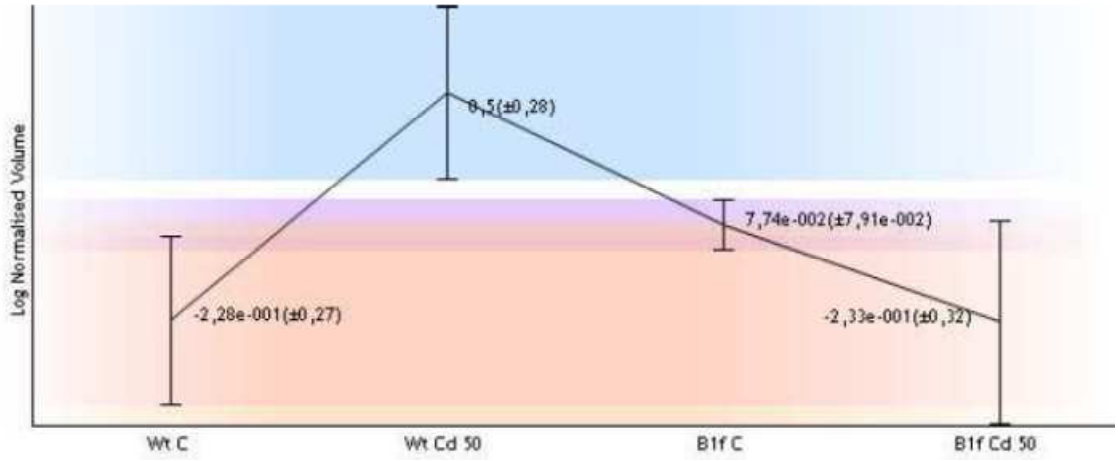

Figure A2 graphic comparing the normalized volumes of the spot 5542 (CA) in each experimental group of the B5H/Wt assay

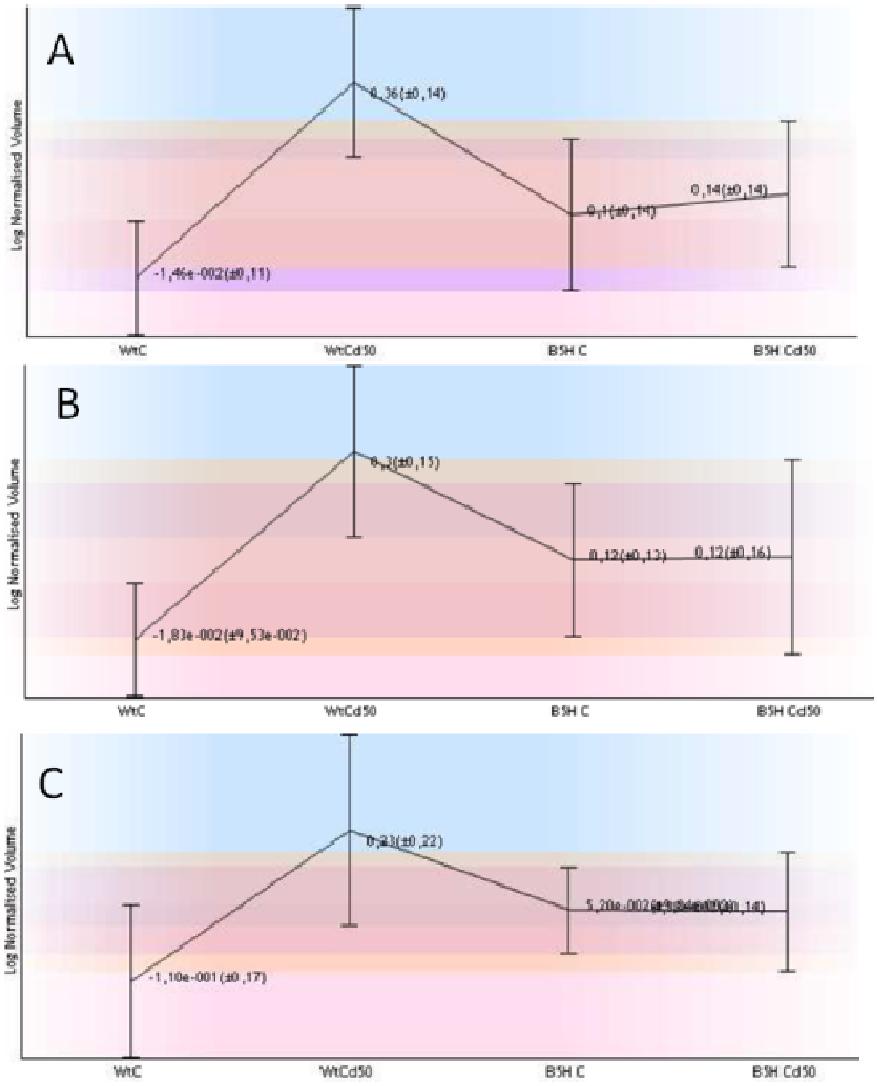

Figure A3: graphics comparing the normalized volumes each experimental group, B5H/Wt assay; A: spot 8512; B: spot 8611; C: spot 8675

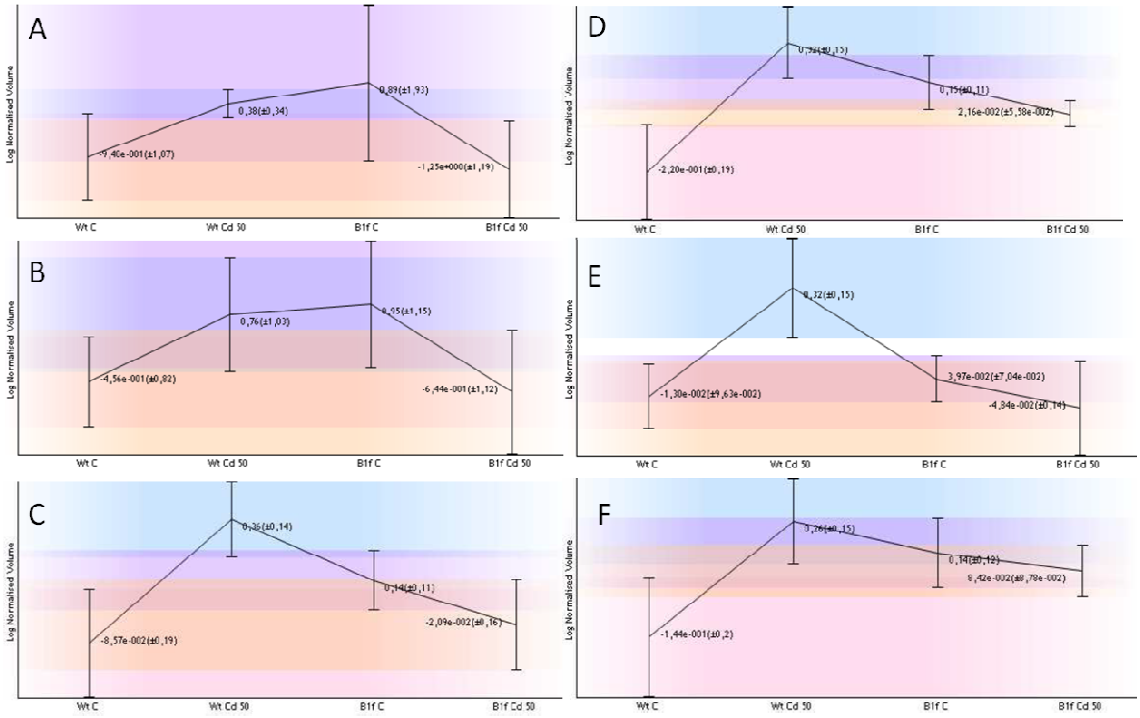

Figure A4: graphics comparing the normalized volumes each experimental group, B1F/Wt assay; A, B and C spots identified as RubisCO large subunit (A: spot 2220; B: spot 2201; C: spot 5470); D, E and F spots identified as RubisCO small subunit (D: spot 5368, E: spot 5379 and F: spot 5837).

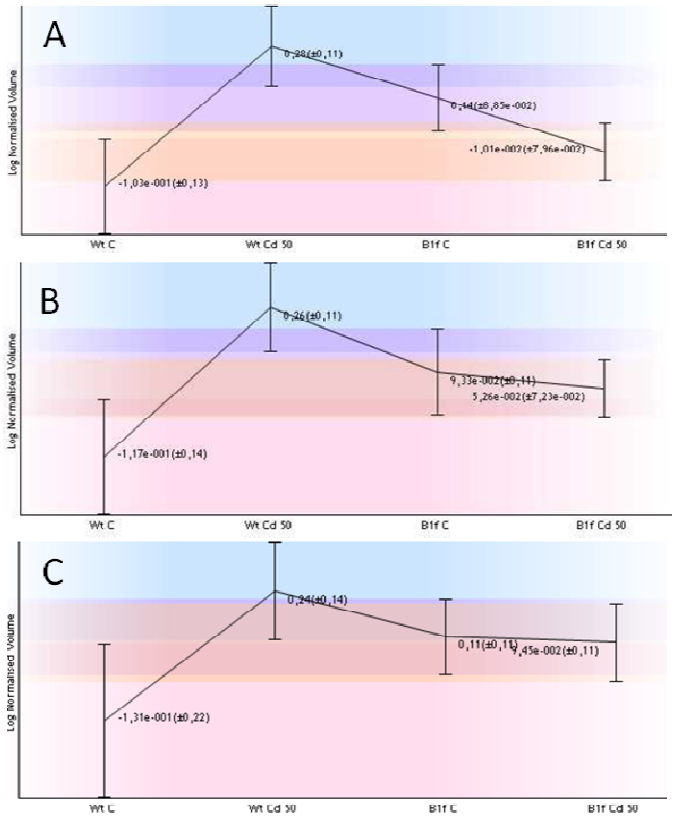

Figure A5: graphic comparing the normalized volumes each experimental group, B1F/Wt assay; A spot identified as RuBisCO activase 1 (spot 5756), B and C spots identified as RubisCO activase 2 (B: spot 5834; C: spot 5798)

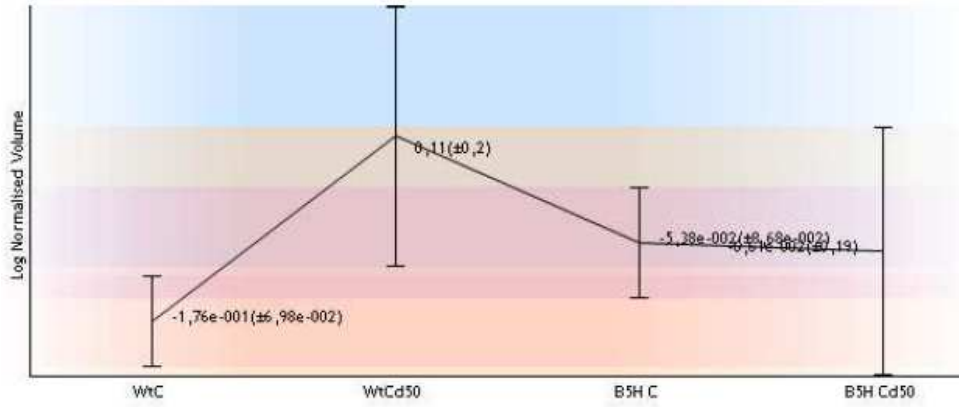

Figure A6: graphic comparing the normalized volumes each experimental group, B5H/Wt assay spot 9174

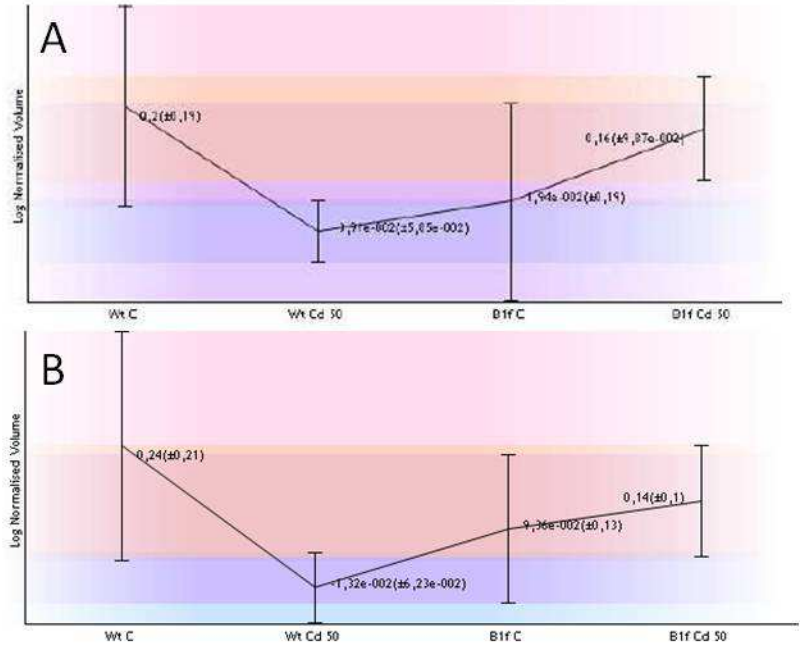

Figure A7: graphic comparing the normalized volumes each experimental group, B1F/Wt assay A: spot 5839; B: spot 5699

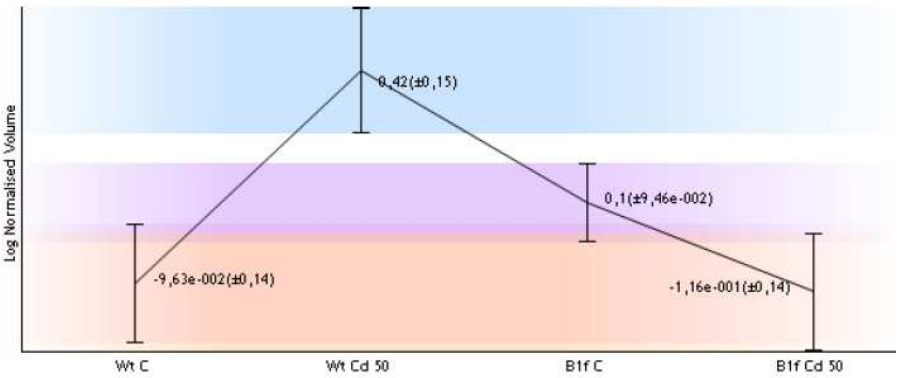

Figure A8: graphic comparing the normalized volumes each experimental group, B1F/Wt assay spot 5495

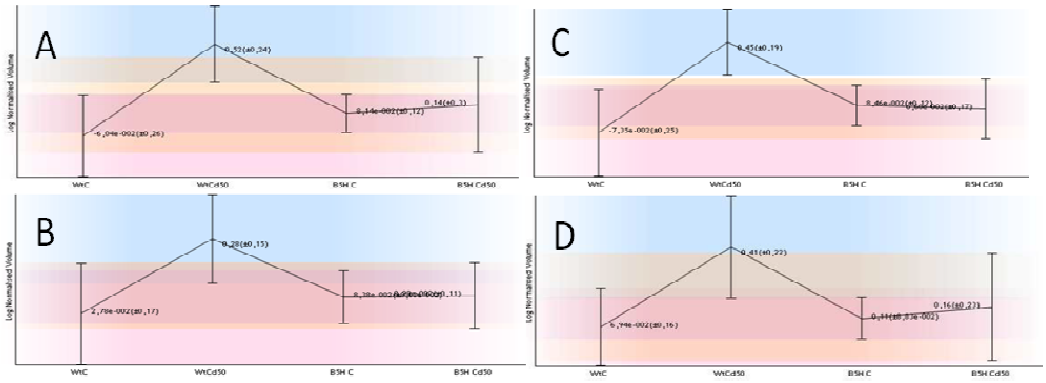

Figure A9: graphic comparing the normalized volumes each experimental group, B5H/Wt assay (A: spot 9237; B: spot 9125; C: spot 9247 and D: spot 8704)

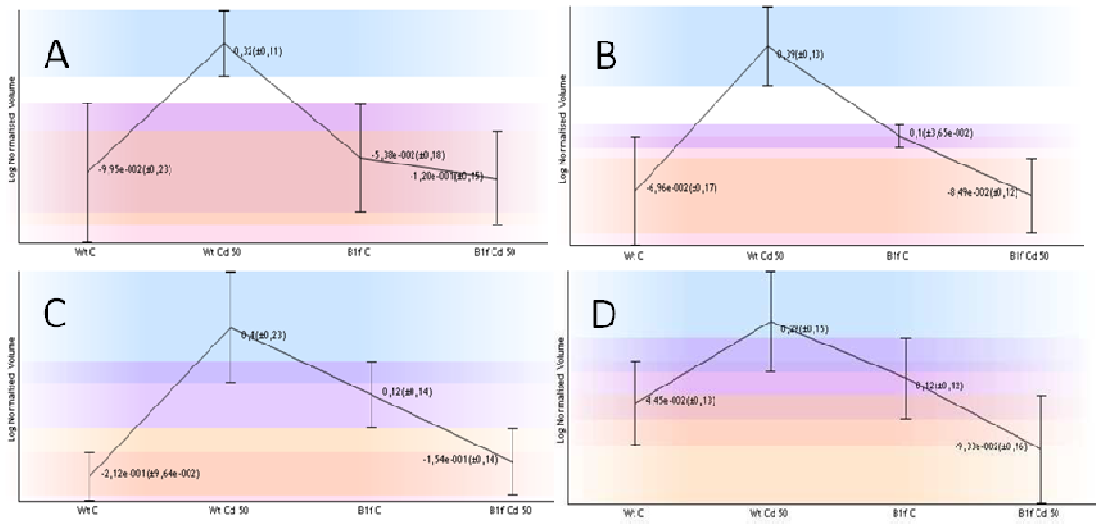

Figure A10: graphic comparing the normalized volumes each experimental group, B1F/Wt assay (A: spot 5624; B: spot 5838; C: spot 5666 and D: spot 5736)

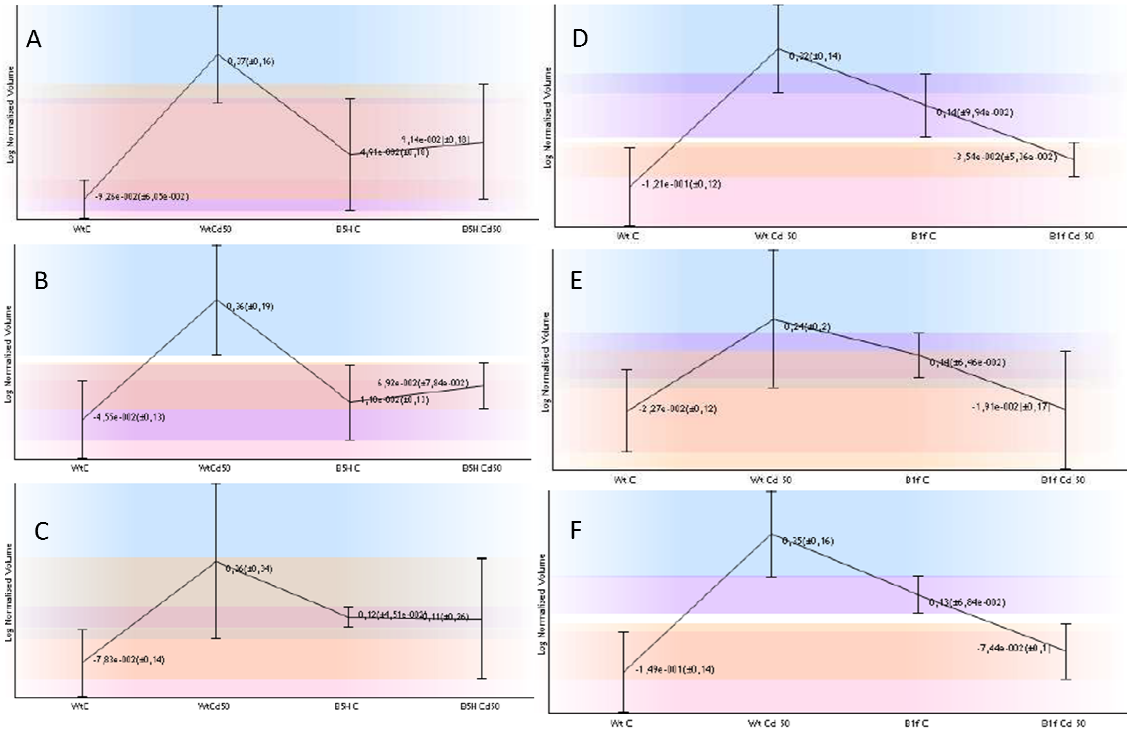

Figure A11: graphic comparing the normalized volumes each experimental group, graphics A, B and C are respective to B5H/Wt assay (A: spot 8919, B: spot 9235 and C: spot 3697) and graphics D, E and F respective to B1F/Wt assay (D: spot 5574, E: spot 5744 and F: spot 5625)

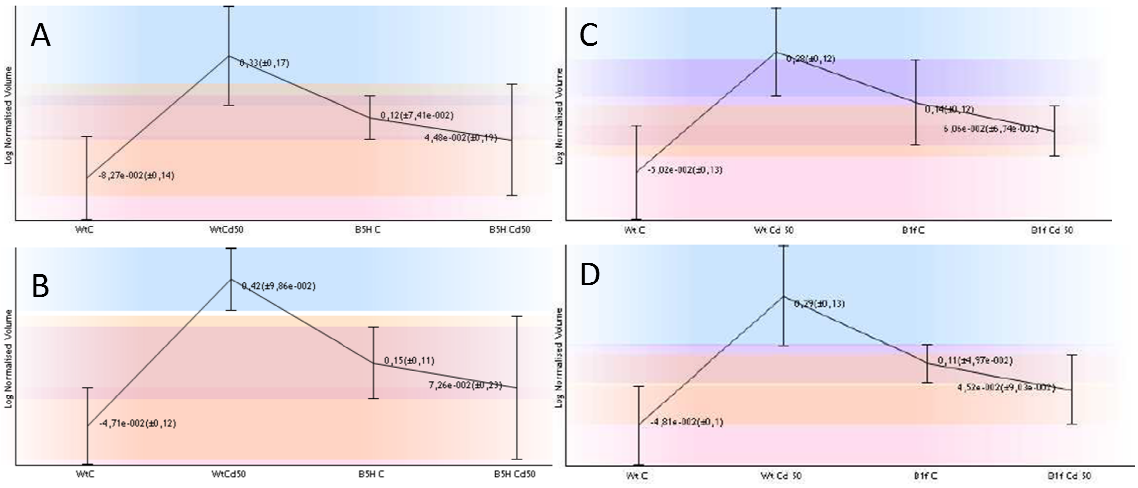

Figure A12: graphic comparing the normalized volumes each experimental group, graphics A and B are respective to B5H/Wt assay (A: spot 9105 and B: spot 8476) and graphics C and D respective to B1F/Wt assay (C: spot 5831 D: spot 5574, E: spot 5803)

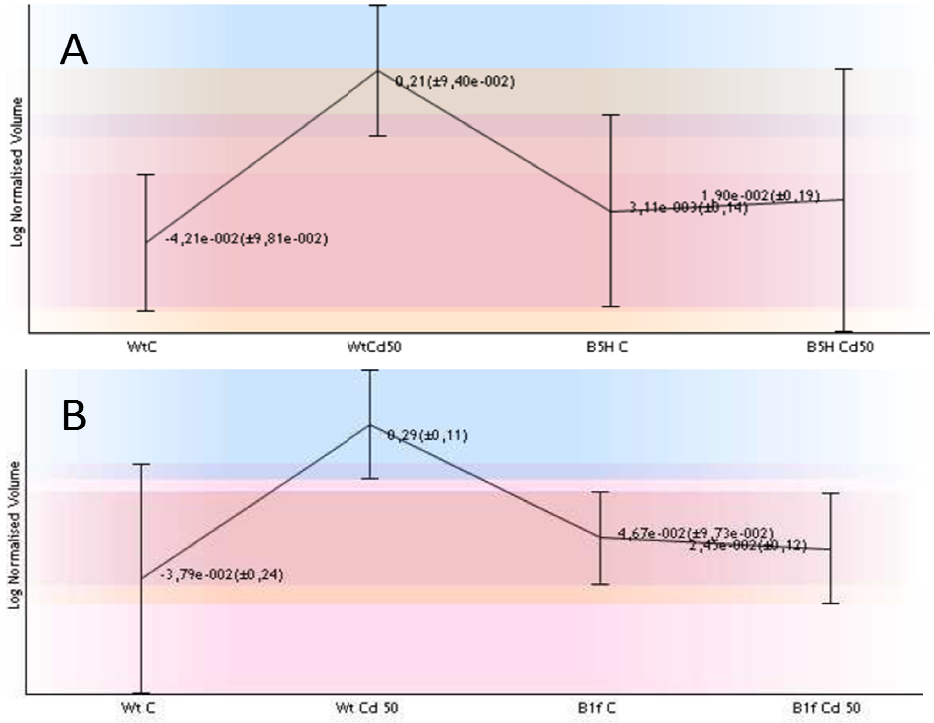

Figure A13: graphics comparing the normalized volumes each experimental group, B5H/Wt assay figure A: 9171 and B1F/Wt figure B: 5674

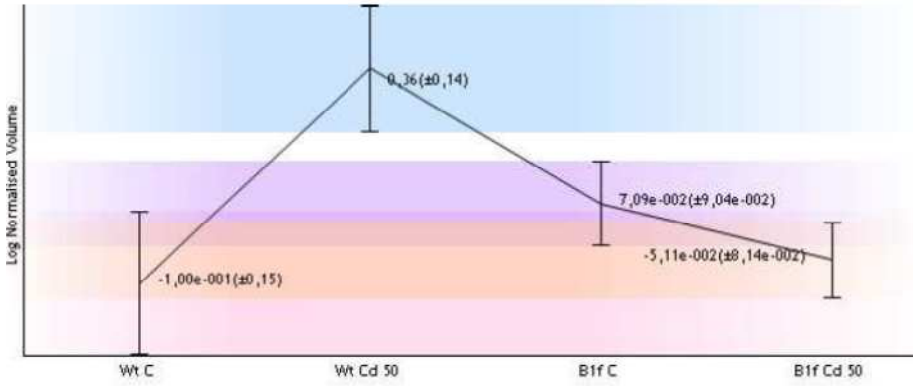

Figure A14: graphic comparing the normalized volumes each experimental group, B1F/Wt assay spot 5731

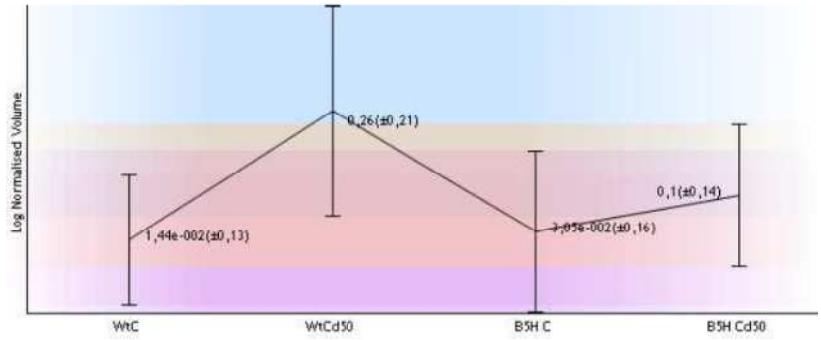

Figure A15: graphic comparing the normalized volumes each experimental group, B5H/Wt assay spot 9146